

Facial-Sketch Synthesis: A New Challenge

Deng-Ping Fan¹, Ziling Huang^{†2}, Peng Zheng^{†3}, Hong Liu^{*4}, Xuebin Qin^{*3} and Luc Van Gool¹

¹Computer Vision Lab, ETH Zürich, Zürich, Switzerland.

²Information and Communication Engineering, University of Tokyo, Tokyo, Japan.

³Computer Vision, MBZUAI, Abu Dhabi, UAE.

⁴Digital Content and Media Sciences Research Division, NII, Tokyo, Japan.

Abstract

This paper aims to conduct a comprehensive study on facial-sketch synthesis (FSS). However, due to the high costs of obtaining hand-drawn sketch datasets, there is a lack of a complete benchmark for assessing the development of FSS algorithms over the last decade. We first introduce a high-quality dataset for FSS, named **FS2K**, which consists of 2,104 image-sketch pairs spanning three types of sketch styles, image backgrounds, lighting conditions, skin colors, and facial attributes. FS2K differs from previous FSS datasets in difficulty, diversity, and scalability and should thus facilitate the progress of FSS research. Second, we present the largest-scale FSS investigation by reviewing **89** classic methods, including **25** handcrafted feature-based facial-sketch synthesis approaches, **29** general translation methods, and **35** image-to-sketch approaches. In addition, we elaborate comprehensive experiments on the existing **19** cutting-edge models. Third, we present a simple baseline for FSS, named **FSGAN**. With only two straightforward components, *i.e.*, facial-aware masking and style-vector expansion, our FSGAN surpasses the performance of all previous state-of-the-art models on the proposed FS2K dataset by a large margin. Finally, we conclude with lessons learned over the past years and point out several unsolved challenges. Our code is available at <https://github.com/DengPingFan/FSGAN>.

Keywords: Facial sketch synthesis, facial sketch dataset, benchmark, attribute, style transfer

1 Introduction

Facial-sketch synthesis (FSS) aims to generate grayscale sketches from RGB images of human faces (image-to-sketch, I2S) or the other way around (sketch-to-image, S2I) [1, 2]. FSS is commonly used by law enforcement or used in surveillance to assist in face recognition and retrieval, based on a sketch drawing from an eyewitness [1]. Entertainment is also used in mobile apps, such as TikTok and Facebook.

In addition, it is an attractive topic in digital entertainment [3]. Research into FSS has achieved significant progress over the past decade.

Different from other face-related datasets, such as those for face recognition [13–15], face detection [16], face key-points detection [17], face alignment [18], and face synthesis [19], which can be manually labelled by annotators with limited training, face sketch datasets are much more difficult to obtain because only professional artists can produce high-quality references. Due to the high costs of obtaining professional

† Contributed equally. * Corresponding authors.

Table 1 Comparison with other FSS datasets.

Dataset	Year	Pub.	Total	Train	Test	Att.	Public	Paired	Resolution
CUFS [1]	2009	TPAMI	606	306	300	✗	✓	✓	200 × 250
IIT-D [4]	2010	BTAS	231	58	173	✗	✗	✓	-
CUFSF [5]	2011	CVPR	1,194	500	694	✗	✓	✓	779.62±15.05 × 812.10±13.92
VIPSL [6, 7]	2011	TCSVT	1,000	100	900	✗	✗	✓	-
DisneyPortrait [8]	2013	TOG	672	-	-	✗	✗	✓	-
UPDG [9]	2020	CVPR	952	798	154	✗	✗	✗	-
APDrawing [10]	2020	TPAMI	140	70	70	✗	✓	✓	512 × 512
FS2K (Ours)	2022	MIR	2,104	1,058	1,046	✓	✓	✓	299.74±95.07 × 273.56±38.67

* Att. = Attributes. In [11] and [12], CUFS is divided into 268 and 338 images for training and testing. For image resolution, we provide the width and height as $W_{avg} \pm W_{std}$ and $H_{avg} \pm H_{std}$, respectively. W_{avg} and W_{std} denote the mean value and standard deviation, respectively.

sketches, existing image-sketch datasets [1, 2, 10] are relatively small with limited diversity. This dataset shortage has limited the development, especially for data-hungry deep learning models.

In addition, how to evaluate FSS remains an open question. Structural similarity (SSIM) [20] is one of the most widely used metrics for evaluating image quality, so it is also typically used to assess the performance of S2I models. Nevertheless, the characteristics of facial sketches are very different from RGB-based facial images, which makes it challenging to apply the current evaluation metrics to I2S tasks. Therefore, a new objective and quantitative metric, which is also highly consistent with human assessment, is needed for benchmarking the FSS task.

Moreover, due to the lack of *high-quality datasets* and *proper evaluation metrics*, different FSS models (*e.g.*, [1, 2]) are usually built and tested on diverse training datasets¹ and with different evaluation methods. Hence, it is not easy to provide fair and comprehensive comparisons. Furthermore, many cutting-edge transformation models (*e.g.*, CycleGAN [21], UNIT [22], Pix2pixHD [23], SPADE [24], DSMAP [25], NICE-GAN [26], and DRIT++ [27]) designed for related image-to-image transfer tasks could potentially be employed in FSS tasks. However, as mentioned above, these models lack performance evaluations for the FSS task because of the shortage of datasets and evaluation metrics. Therefore, thorough comparisons and assessments of FSS-related models on a standard FSS dataset with unified evaluation metrics are long overdue. To this end, we have introduced and maintained an online paper list (<https://github.com/DengPingFan/FaceSketch-Awesome-List>) to track the progress of this fast-developing field.

1.1 Contributions

Our goal is to solve the discussed issues (*i.e.*, limited datasets, metrics, and benchmarks) and further contribute to a new challenge for the FSS community. The main contributions are as follows:

- 1) **FSS Dataset.** We build a new high-quality FSS dataset, termed **FS2K**. It is the largest (see Table 1) publicly released FSS dataset,² consisting of 2,104 image-sketch pairs with a wide range of image backgrounds, skin patches, sketch styles, and lighting conditions. In addition, we also provide extra attributes, *e.g.*, *gender*, *smile*, *hair style*, *etc.*, to enable deep learning models to learn more details.
- 2) **FSS Review and Benchmark.** We conduct the largest-scale FSS study, reviewing 89 representative approaches, including 25 methods using handcrafted features, 29 models for the general transfer task, and 35 I2S transfer algorithms. Based on our FS2K, we adopt the SCOOT metric [29] and conduct a rigorous evaluation of 19 state-of-the-art models from the perspective of content and style.
- 3) **FSS Baseline.** We design an efficient GAN-based baseline, termed **FSGAN**, which consists of two simple core components, *i.e.*, facial-aware masking and style-vector expansion. The former is utilized to restore details of the facial components, while the latter is adopted to learn different face styles. FSGAN serves as a unified baseline model for both I2S and S2I tasks (Fig. 1) on our newly built FS2K dataset. Our project is available at <https://github.com/DengPingFan/FSGAN>.

¹Because they want to learn a different style of sketches.

²Establishing an FSS dataset drawn by professional artists is more challenging than other face datasets, *e.g.*, face attribute datasets [28], which is why the largest existing FSS dataset, *i.e.*, CUFSF [5], has only ~1K images in the past 13 years. Although FS2K is only ~2 times larger than CUFSF, we still took one year to create such a high-quality dataset.

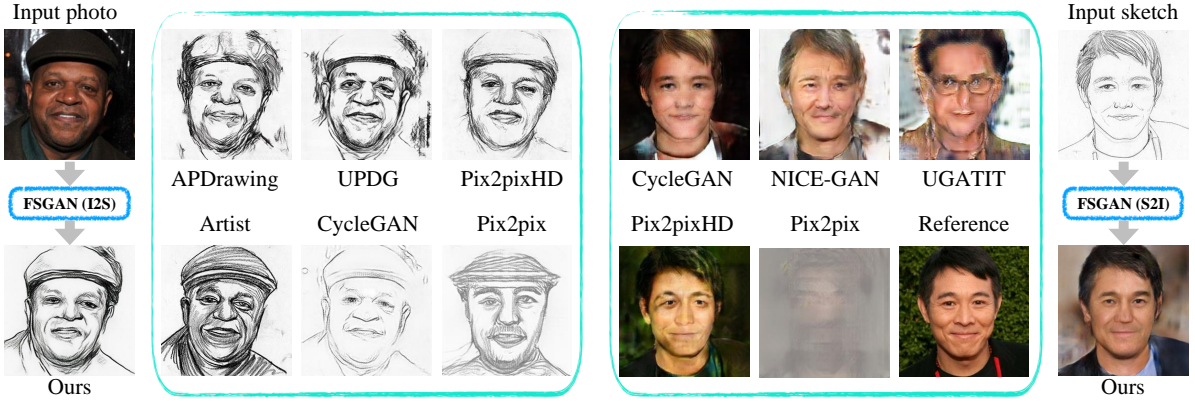


Fig. 1 **Left:** Our FSGAN (I2S) learns from artist drawings and intelligently turns an input photo into a vivid face sketch. In contrast, the five cutting-edge style transfer approaches cannot obtain visually appealing results. Only UPDG [9] and Pix2pixHD [23] perform relatively well, but they generate worse content and style than FSGAN. **Right:** Given a sketch, our FSGAN (S2I) can also transform the input into a vivid facial photo. Meanwhile, the results from the five representative deep learning models are either structurally damaged (*i.e.*, CycleGAN [21], NICE-GAN [26], and UGATIT [30]) or blurry (*i.e.*, Pix2pix [31]). More results can be found in Fig. 8–11.

4) **Discussions and Future Directions.** In addition to an overall performance assessment, we also conduct an attribute-level evaluation, present detailed discussions, and explore some promising future directions.

2 Related Works

This section first conducts a complete literature review of the existing FSS datasets. Then, in the second part, we discuss the taxonomy of facial-sketch synthesis and highlight particularly innovative and successful approaches for this task, including traditional facial synthesis, image-to-image translation, neural style transfer, and deep photo-sketch synthesis. The taxonomy of facial-sketch synthesis is shown in Fig. 3. A summary of the models, including their key innovations, datasets, code links, and citation information, can be found in Table 2 and Table 3.

2.1 Dataset

We outline four classical datasets for the FSS task, *i.e.*, CUFS [1], IIIT-D [4], CUFSF [5], VIPSL [7], and three portrait sketching datasets [8–10], which are the basis for building most FSS models [32].

CUFS [1] is one of the earliest and most commonly used datasets. It contains 606 photo-sketch pairs, which include 123 samples from the AR face database [33], 188 samples

from the CUHK student database, and 295 samples from the XM2VTS database [34]. A sketch drawn by an artist and a corresponding photo are provided for each sample. Each photo is taken in a frontal pose under normal lighting conditions and maintains a neutral expression. All three sub-databases use solid backgrounds, *e.g.*, cyan, white, blue, *etc*. However, real-world scenes are complex and diverse, and it is difficult to guarantee that photos will be captured in such a fixed environment. Besides, the sketches in this dataset were created by the same artist, so they are of limited style.

CUFSF [5] is a commonly used database for assessing the performance of FSS models. It contains 1,194 photo-sketch pairs, collected from the FERET database [35]. An artist drew all sketches after viewing the corresponding photo. CUFSF has a similar photo collection environment to CUFS but is more challenging. Because the photos in the dataset undergo illumination changes, each face has low contrast with the background, and each sketch contains exaggerated shapes.

VIPSL [7] contains 200 face photos collected from the FRAV2D [36], FERET [35], and Indian face databases [7]. Unlike CUFS and CUFSF, VIPSL has five sketches for each face, drawn by five artists with different styles, while viewing the same photo under the same conditions as CUFS.

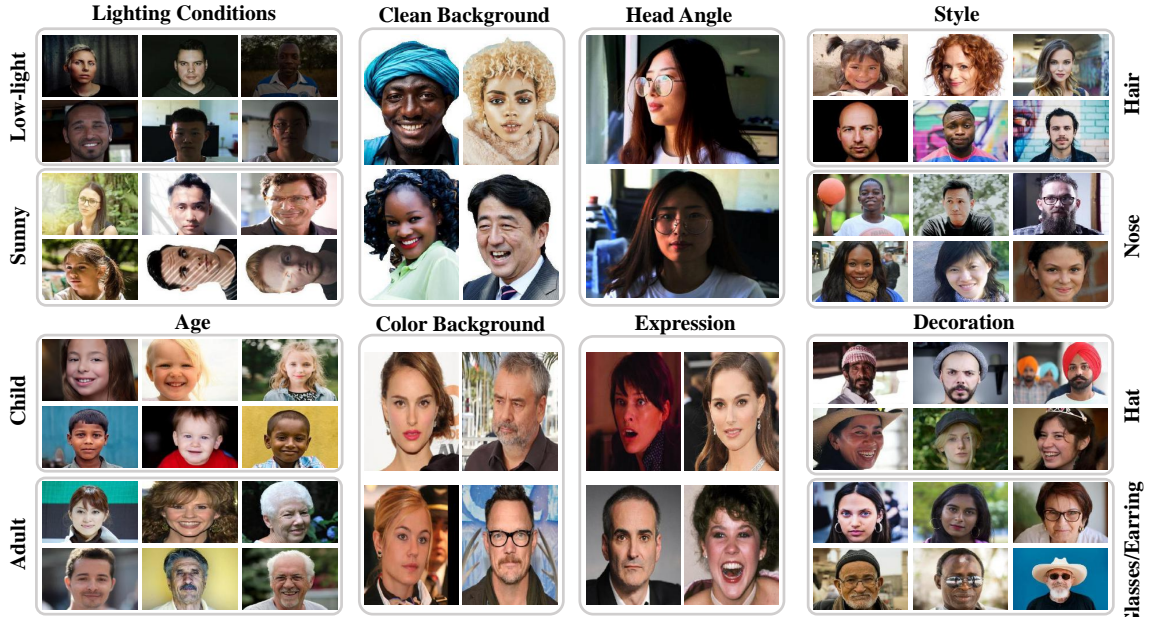


Fig. 2 Representative image samples from our FS2K. The collected images depict diverse scenes according to different selection criteria, such as various lighting conditions (*i.e.*, low-light, sunny), ages (*i.e.*, child or adult), backgrounds (*i.e.*, clean or colored), head angles, facial expressions (*e.g.*, serious, smiling, and laughing), hair styles (*e.g.*, black, blonde, long, and short), and accessories (*i.e.*, hat or earrings).

IIIT-D [4, 37] consists of three types of sketch databases, including a viewed sketch database, a semi-forensic sketch database, and a forensic sketch database. All photos are derived from the CUHK student database and IIIT-Delhi Sketch database [4]. The first viewed sketch database contains 238 sketch-digital image pairs, with all sketches drawn by the professional artist based on a given photo. The second sub-database has 140 sketch-face image pairs, where all the sketches are drawn by memory after the artist has observed the corresponding photo. The third forensic sketch database consists of 190 sketches that a sketch artist draws according to the description of an eyewitness based on their recollection of a crime scene. IIIT-D contains multiple styles of sketch portraits, making it more challenging. However, obtaining forensic sketches is tricky since they are usually derived from law enforcement.

Portrait Sketching Dataset. Yi *et al.* [9, 10] provided two datasets that simulate artistic portrait drawing (APDrawing). The first dataset [10] contains 140 pairs of face photos and corresponding sketch portraits drawn by a single portrait artist. This was later extended to a larger dataset in [9], with 952 face photos and 625

portrait sketches. Of the collected photos, 220 are from three famous painters, and the remaining 212 photos are from a photography website.³ It is worth noting that the photos and portraits in this dataset are not paired. Disney Research published a portrait dataset [8] composed of 24 faces from the face database [38] and 672 sketches from seven artists under four levels of abstraction. Besides, they also provided each stroke as a transparent bitmap to be used later to create new sketches.

Unlike existing datasets, we provide a more challenging, high-quality, and attribute-annotated dataset, which is currently the largest FSS dataset. The new dataset contains 2,104 pairs of photos and sketches, 1,058 used for model training, and the remaining for evaluation. The strengths of our FS2K include multiple drawing styles, highly accurate alignment between sketches and photos, multiple attribute information, complex backgrounds, *etc.* Detailed comparisons of the datasets are shown in Table 1.

³<https://vectorportal.com/>

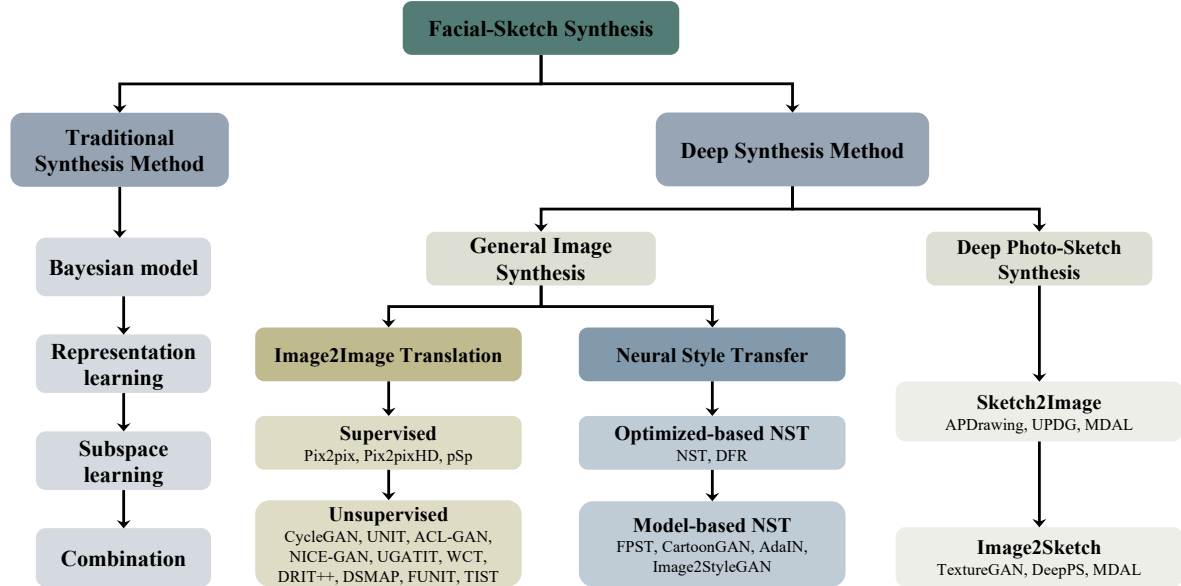


Fig. 3 A taxonomy of facial-sketch synthesis and the representative methods.

2.2 Traditional Facial Synthesis

Researchers have used heuristic image transformations to interactively or automatically synthesize facial sketches [3, 39–43] in the early years. However, these methods tend to generate artificial and inexpressive sketches that lack artistic style. Therefore, in recent years, more attention has been focused on learning-based facial synthesis schemes, whose taxonomy is shown in Fig. 3. These can be categorized into Bayesian inference models, representation learning models, subspace learning models, *etc.*

2.2.1 Bayesian Inference Models

Bayesian inference exploits evidence to update the states of the sketch components over probability models, which has been widely used in FSS [44]. In [45], Chen *et al.* first introduced an example-based facial-sketch synthesis system that uses a non-parametric sampling algorithm to learn subtle sketch styles. Later, the embedded hidden Markov model [46] was used to model the non-linear relationships in photo-sketch pairs, followed by a selective ensemble strategy to generate facial sketches [47]. Wang and Tang [1] followed a similar idea but considered face structures across different scales, using a multi-scale Markov Random Field (MRF) to build the relationships between photo-sketch

pairs. Xu *et al.* [48] proposed a hierarchical compositional model that considers the regularity and structural variation of faces. These methods have made significant progress in generating sketches, but they only consider simple controlled conditions, ignoring variations in lighting and pose. Zhang *et al.* [49] addressed this issue by simultaneously considering patch matching, intensity compatibility, gradient compatibility, and shape priors, resulting in better visual effects. However, MRF-based models have two main drawbacks: (1) they struggle to synthesize unseen facial information and (2) their optimization is NP-hard. Zhou *et al.* [50] used Markov weight fields and cascaded decomposition to build a robust facial synthesis system, using a linear combination of candidate patches to approximate new sketch patches. Wang *et al.* [51] built a non-parametric model to transform a photograph into a portrait painting, where an MRF is used to enhance the spatial coherence of the style parameters, and an active shape model and a graph-cut model are used to learn the local information of facial features. Wang *et al.* [52] presented a transductive learning method to synthesize facial sketches, which employs an on-the-fly optimization process to minimize the loss of the given test samples. Peng *et al.* [53] designed a superpixel method built on the Markov model to improve the flexibility without dividing

the photo into regular rectangular patches. Then, they not only used the Markov network to model the relationships between image patches but also retained many visual aspects of the cues (such as edges) through multiple visual features [54].

2.2.2 Subspace Learning Models

Subspace learning has been widely studied in the FSS task [44], which learns a low dimensional manifold space embedded in a high dimensional space [55]. Tang and Wang [56–58] proposed a series of example-based approaches based on the linear eigen-transformation method. These methods are global linear systems, and they cannot fully explain the relationships between photo-sketch pairs because such a transformation is not a simple linear relationship. Liu *et al.* [59] used the LLE to handle this problem, making photo and sketch patches have manifolds with similar local geometric shapes in two different image spaces. However, pseudo-image generation and representation learning are divided into two independent processes, leading to sub-optimal results. Huang and Wang [60] proposed a joint learning framework, which contains domain-specific dictionary learning and subspace learning.

2.2.3 Representation Learning Models

Sparse coding and dictionary learning, *a.k.a.* representation learning, are used for the FSS task [44]. Ji *et al.* [61] demonstrated that personalized features are not effectively captured through the synthesis process. As such, several works [61–63] use different regression models, such as k-NN [61], Lasso [61], multivariate output regression [62], and support vector regression [63], to build the transformation between photos and sketches. To improve the quality of the generated facial sketches, Wang *et al.* [6, 7] used local linear embedding (LLE) [64] to estimate an initial sketch or photo and then introduced a sparse multi-dictionary representation model that can focus on high-frequency and detailed information. However, most representation-based models assume that the same representations are shared by the source input and the target output, limiting a particular style’s local structures in the synthesis process. To relax this constraint, Wang *et al.* [65] introduced a semi-coupled

dictionary learning method, in which a linear transformation is used to bridge the gap between two different domain-specific representations. Gao *et al.* [7] also took a two-step algorithm [63] into consideration, presenting a selection scheme to generate the initial pseudo-images and introducing a sparse-representation-based enhancement (SRE) to synthesize sketches.

2.2.4 Combination Models

Recently, some works have explored combination models, which combine different machine learning models, *e.g.*, combing Bayesian inference and subspace learning methods. Berger *et al.* [8] proposed a model to simulate the styles of the different artists and the process of abstraction, which can be used for facial-sketch synthesis. Song *et al.* [66] introduced a real-time FSS method, which first uses a k-NN algorithm to find the top-k similar local patches. Then a linear combination is used to compute the corresponding sketch image and image denoising technology is adopted to enhance the visual quality. However, the model [66] is still time-consuming due to the k-NN process, so Wang *et al.* [67] addressed this problem by replacing offline random sampling with an online scheme that is further combined with a recognition weight representation. Most existing traditional methods are entirely dependent on the scale of the training data, so Zhang *et al.* [68] presented a robust model trained on a template stylistic sketch. The model includes representation learning, MRF, and a cascaded model. Li *et al.* [69] proposed a free-hand sketch synthesis method, combining a perceptual grouping model with a deformable stroke model. The work in [70] introduces an adaptive learning method that combines representation learning and a Markov network. Men *et al.* [71] proposed a common framework for interactive texture transfer with structure guidance. Their model implements the synthesis process dynamically using multiple channels, including structure extraction, structure propagation, and guided texture transfer.

2.3 General Image Synthesis

Deep facial-sketch synthesis belongs to the task of image generalization. Therefore, general image synthesis methods, such as image-to-image translation and neural style transfer, can also be

used to generate facial sketches. We will overview various cutting-edge transformation models.

2.3.1 Image-to-Image Translation

Image-to-image translation (I2I) [72] is a hot topic in computer vision and machine learning. The goal is to transform the input image from a source domain to a different target domain while retaining the intrinsic source content and transferring the extrinsic target style. Current I2I models are typically built on a generative adversarial network (GAN) [73]. They can be generally categorized into supervised and unsupervised I2Is.

Supervised I2I. Supervised I2I uses aligned image pairs as the source and target domains to learn a transformation model that can convert the source image into the target image. One representative I2I method is Pix2pix [31], which applies a conditional GAN (cGAN) [74] to the task. The main difference from the original cGAN is that the generator in Pix2pix is a U-Net [75]. However, Wang *et al.* [23] observed that the adversarial training in Pix2pix is unstable, preventing the model from generating high-resolution images. Therefore, they extended the original Pix2pix with a new feature matching loss, which can generate high-resolution images of size 2048×1024 . Zhu *et al.* [76] proposed the BicycleGAN, which includes a conditional VAE and a conditional latent regression GAN, to resolve the collapse problem and achieve improved performance. Furthermore, to reduce the loss of semantic information in the Pix2pixHD model [23], Park *et al.* [24] introduced a SPADE-based generator, which adds spatially-adaptive normalization into the generator of Pix2pixHD so as to enhance the semantic information throughout the network.

Unsupervised I2I. Collecting paired data is not practical because it is labor-intensive. Therefore, several unsupervised I2I models have been proposed to train two different generative networks under the constraint of a cycle-consistency loss. If we convert a zebra image to a horse image and then back to a zebra image, we should get the same input image back. Examples include CycleGAN [21], DiscoGAN [77], and DualGAN [78]. Later, Liu *et al.* [22] proposed an unsupervised I2I model (UNIT),

in which the same latent code in a shared latent feature space can represent image pairs in different domains. Kim *et al.* [30] later proposed a novel attention module with a new normalization function, which they integrated into a GAN model to supervise texture and shape variations flexibly. By rethinking the standard GAN model, Chen *et al.* [26] proposed a NICE-GAN with the key idea of coupling discriminators and encoders, *i.e.*, reusing the discriminator parameters for encoding the input. Zhao *et al.* [79] proposed ACL-GAN, which utilizes a new adversarial consistency loss instead of a cyclic loss to emphasize the commonality between the source and target domains. To improve the content representation ability, Chang *et al.* [25] proposed DSMAP to leverage the relationship between content and style. Specifically, the model maps content features from a shared domain-invariance feature space into two separate domain-specific features. Furthermore, DRIT++ [27] uses two image generators, two content encoders, a content discriminator, two attribute encoders, and two domain discriminators to embed an image into a domain-invariant content space and a domain-specific attribute space. Besides, Jiang *et al.* [80] proposed two-stream I2I translation (TSIT) to learn both semantic structural features and stylistic features and then fuse the feature maps of the content and style in a coarse-to-fine manner. More recently, Zhang *et al.* [81] proposed a CoCosNet for exemplar-based image translation, which contains two sub-networks. The first embeds the inputs from different domains into a feature domain that depends on the semantic correspondence. Meanwhile, the second uses a series of denormalization blocks to progressively synthesize the target images. Zhou *et al.* further extended CoCosNet with full-resolution semantic correspondence learning [82], with the main difference being the use of a regular and GRU-based propagation applied iteratively at each semantic level. More recently, Chen *et al.* [83] proposed a SofGAN, which decouples the portrait feature into a geometric feature and a texture feature. These two features are then fed into two network branches. The first branch is a hyper network to decode the geometric feature into the weight of the SOF net that represents the semantic occupancy field (SOF) among 3D space. Then, a segmentation map is rendered via

a ray-casting-marching scheme using the output features of the SOF net. The second branch is a texture transformation of each semantic region using a GAN generator with a style code sampled from the texture space. Finally, a novel Semantic Instance Wise (SIW) StyleGAN module is used to stylize the generated segmaps and output a photorealistic portrait regionally.

2.3.2 Neural Style Transfer

Neural style transfer (NST), which aims at generating visually appealing images via neural networks, has been introduced into the FSS task [84]. Specifically, NST is used to render a content image in different styles. NST methods can be categorized into optimization-based methods and model-based methods.⁴

Optimization-based methods. The online NST algorithm iteratively updates a given input image to match the desired CNN features, including the photo's content and artistic style information. Gatys *et al.* [87, 88] made the first contribution to this field, using a classical CNN (*i.e.*, VGG [89]) to render an image with famous painting styles. Besides, StyleGAN [90] uses a latent space to maintain consistent results for image synthesis. However, it is challenging to achieve promising results under the given conditions. Recently, Abdal *et al.* [91] integrated the classical NST [87, 88] into the StyleGAN model, using NST to project the input image into the latent space defined in StyleGAN. Then, Kotovenko *et al.* [92] further enhanced the classical NST [87, 88] by optimizing parameterized brushstrokes, which is built on a simple differentiable rendering mechanism.

Model-based methods. Optimization-based online methods achieve satisfactory results, but there are still some limitations. One major drawback is the slow computational speed and high cost of online iterative optimization. To address this issue, several works introduce a feed-forward network to mimic the optimization objective of style transfer [84].

End-to-end models can be divided into those that design a basic deep neural architecture and those that introduce a new loss function. For basic architectures, Johnson *et al.* [93] took advantage of the benefits of the neural network and optimization-based NST model and proposed a method for training a feed-forward network using a new perceptual loss. TextureNet [94] follows a similar idea but with different neural network architecture. Both [93] and [94] are real-time style transfer methods. Chen and Schmidt [95] introduced a style swap operation to exchange the patches with visual context and those with style, further formulating a new optimization objective that aims to learn an inverse neural network for arbitrary style transfer. In terms of methods based on the loss function, CartoonGAN [85] was presented to transfer real-world photos into cartoon-style images. It consists of two novel loss functions designed to preserve clear edge information and cope with the stylistic difference between photos and cartoons.

Recently, several researchers have begun using a small number of parameters to characterize each style, *i.e.*, changing the parameters in the normalization layer for style transfer. Dumoulin *et al.* [121] made the exciting observation that normalization layers can reflect the statistical properties of different styles. Therefore, they scaled and shifted the parameters in these layers while keeping the convolutional parameters unchanged to obtain better NST. Further, they introduced flexible conditional instance normalization, enabling style transfer by simply changing the normalization parameters online. Ulyanov *et al.* [122] improved their previous TextureNet [94] by simply applying normalization to each image rather than a batch of images, which they called instance normalization. Moreover, they also demonstrated that the style transfer network with instance normalization could converge faster than that with batch normalization while achieving visually better results. Later, Huang and Belongie [123], following a similar idea, introduced adaptive instance normalization into the GAN model, aligning the content and style features. Li *et al.* [124] further used the first few layers of a pre-trained VGGNet [89] to extract the feature representation. However, they replaced the AdaIN layer with whitening and coloring transformations, enabling

⁴Note that some related works belong to the general GAN-based model, such as CartoonGAN [85] and pSp [86]. These GAN models can be used for either neural style transfer or image-to-image translation. Since we do not make a specific review of the generalized GAN model, we classified a few GAN models into the neural style transfer task as a quick overview of these methods.

Table 2 Summary of popular related works. These can be categorized into three types: *Traditional Facial Synthesis*, *General Image Synthesis*, and *Deep Image-to-Sketch Synthesis*. **Publ.**: Publication information. **Year**: Publication year. **Code**: The link of the corresponding open resources. **Components**: The key components of each model. **Dataset**: A = TU-Berlin Sketch Dataset [96], B = Disney Portrait Dataset [8], C = FERET [35], D = AR [33], E = Self-Collected, F = MSCOCO [97], G = ImageNet [98], I = CelebA [28], L = DTD [99], P = Wikiart [100], Q = Cityspace [101], R = CMP Facades [102], S = Edge2photo [103, 104], U = Day2night [105], V = MNIST [106], Y = CUFS [1], Z = Caltech-200 Bird [107], AC = CelebAHQ [108], AD = NYU Indoor RGBD dataset [109], AE = ADE20K [110], AK = QMUL-Shoe-Chair-V2 [111], AL = QuickDraw dataset [112], AP = Yosemite [21], AQ = cat2dog [27], AR = Flickr Landscapes [24], AS = APDrawing Dataset [2], AT = Anime Faces of Getchu [113], AU = Selfie2anime [30], AV = horse2zebra [21], AW = photo2vangogh [21], AX = photo2portrait [27], BH = Berkeley Deep Drive [114], BI = SYNTHIA dataset [115], BJ = UPDG [9], BK = DeepFashion [116], BU = FFHQ [90], BV = DIV2K [117], BW = LHI [118], BX = VIPS [6], BY = IIIT-D [4], BZ = Map2Aerial [31], CB = StandfordCars [119], CH = LSUN [120], CU = CUFSF [5]. **Assist.**: Assistant Information, *e.g.*, Bm.= Background map, Sm.= Segmentation map, Fl.= Facial landmark, Sv.= Style vector, Cm.= Color map, Attri.= Facial Attribute, Km.= Keypoint map, Tp.= Texture patch. **Cite.**: Google citation statistics are from 2022-05-21.

#	Model	Publ.	Year	Code	Components	Dataset	Assist.	Cite.
Traditional Facial Synthesis								
1	EFSGNS [45]	ICCV	2001	-	Active Shape Model, Non-parametric Sampling	E	-	160
2	Nonlinear [59]	CVPR	2005	-	Local Linear Preserving, Eigentransform	Y	-	398
3	E-HMM [47]	TCSV	2008	-	Embedded Hidden Markov Model, Selective Ensemble	Y	-	165
4	HCM [48]	PAMI	2008	-	Graph, Minimum Description Length	C, D, BW, E	-	93
5	MRF [1]	PAMI	2009	Code	Multi-scale Markov Random Fields	Y	-	872
6	LPR [49]	ECCV	2010	-	Local Evidence Function, Patch Matching, Shape Prior, MRF	Y	-	120
7	LRM [61]	ICIG	2011	-	Local Regression, kNN	Y	-	19
8	MOR [62]	HCI	2011	-	Multivariate Output Regression	Y	-	22
9	MDSR [6]	ICIG	2011	-	LLE, Dictionary Learning, Sparse Representation	Y, BX	-	55
10	SVR [63]	ICIP	2011	-	Support Vector Regression	Y, BX	-	41
11	SCDL [65]	CVPR	2012	-	Sparse Coding, Semi-coupled Dictionary Learning	Y	-	613
12	MWF [50]	CVPR	2012	-	Markov Weight Fields, Cascade Decomposition	Y, E	-	173
13	SI [7]	TCSV	2012	-	Sparse Neighbor Selection, Sparse-Representation Enhance	Y, BX	-	185
14	SAPS [8]	TOG	2013	-	Edge Detection, Shape Deformation	B	-	116
15	FESM [51]	BMVC	2013	-	Markov Random Field, Graph-cut	E	-	22
16	Transductive [52]	TNNLS	2013	-	Probabilistic graph model, Transductive Learning	Y, CU	-	167
17	CDFSL [60]	ICCV	2013	-	Coupled Dictionary and Feature Space Learning	Y	-	177
18	REB [66]	ECCV	2014	Project	kNN, Linear Estimation, Sketch Denoising	Y, D	-	124
19	RobustStyle [68]	TIP	2015	-	Sparse Representation, Multi-scale Selection	Y, E	-	49
20	SPP [53]	TCSV	2015	Project	Superpixels, Markov Networks	Y, CU, BY	-	45
21	MR [54]	TNNLS	2016	-	Markov Networks, Edge Enhancement, Alternating Opt.	Y, BY	-	107
22	DSM [69]	IJCV	2017	Project	Perceptual Grouping, Deformable Stroke Model	A, B	-	37
23	AR [70]	NC	2017	-	Adaptive Representation, Markov Networks	Y	-	10
24	RS [67]	PR	2018	-	Offline Random Sampling, Locality Constraint	Y, CU	-	96
25	CFITT [71]	CVPR	2018	Github	PatchMatch, Guided Texture Transfer	E	Sm.	19
General Image Synthesis								
26	NST [87, 88]	CVPR	2016	Github	Parametric Texture Mode, Representation Inversion	E	-	3853
27	FNS [93]	ECCV	2016	Github	Image Transformation and Loss Network, Perceptual Loss	F	-	7038
28	TextureNet [94]	ICML	2016	Github	Generator Network, Descriptor Network,	E	-	813
29	FPST [95]	NeurIPS	2016	Github	CNN, Style Swap, Inverse Network	F, P	-	285
30	CIN [121]	ICLR	2017	Github	Conditional Instance Normalization	G, E	-	838
31	ITN [122]	CVPR	2017	Github	Instance Normalization, Julesz Generator Network	E	-	546
32	AdaIN [123]	ICCV	2017	Github	Adaptive Instance Normalization	F, P	-	2123
33	WCT [124]	NeurIPS	2017	Github	Multi-level Stylization, Whitening and Coloring Transforms	F, L	-	578
34	CartoonGAN [85]	CVPR	2018	Github	GAN, Semantic Content Loss, Edge-promoting Loss	E	-	227
35	I2SGAN [91]	CVPR	2019	Github	StyleGAN, Embedding	AC, BU	-	389
36	RST [92]	CVPR	2021	Github	Differentiable Renderer, Brushstrokes Parameterization	E	-	10
37	b5p [86]	CVPR	2021	Github	StyleGAN, Disentangled Latent Feature, Map2Style	AC, BU	-	194
38	Pix2pix [31]	CVPR	2017	Github	Generator with Skip, PatchGAN	A, G, Q, R, S, U, BZ	-	13244
39	CycleGAN [21]	ICCV	2017	Github	Map Functions and Discriminators, Cycle Consistency Loss	A, G, Q, R, S, U, AV, AW	-	12734
40	DualGAN [78]	ICCV	2017	Github	Trained in Closed Loop, Reconstruction Loss	R, U, Y, CU, BZ, E	-	1554
41	DiscoGAN [77]	ICML	2017	Github	GAN with a Reconstruction Loss	CI, K, I, AH, S	-	1714
42	BicycleGAN [76]	NeurIPS	2017	Github	cVAE-GAN, cLR-GAN	R, S, U, BZ	-	1114
43	UNIT [22]	NeurIPS	2017	Github	Common Latent Space, VAEs, Cycle-consistency, GAN	G, I, Q, V, W, X, BI	-	2138
44	Pix2pixHD [23]	CVPR	2018	Github	Coarse-to-fine Generator, Multi-scale Discriminator	Q, AD, AE, AF	-	2527
45	MUNIT [125]	ECCV	2018	Github	Content/Style Encoder, AdaIN, Decoder	A, S, AP, BI, E	-	1615
46	SPADE [24]	CVPR	2019	Github	Spatially-Adaptive Normalization, Pix2pixHD	F, Q, AE, AR	Sm.	1362
47	U-GAT-IT [30]	ICLR	2020	Github	Attention map, Adaptive Layer-Instance Normalization	AU, AV, AW, AX	-	248
48	CoCosNet [81]	CVPR	2020	Github	Cross-domain Correspondence, Translation Network	AE, AC, BK	-	104
49	TSIT [80]	ECCV	2020	Github	Multi-scale Feature Normalization, Two-stream Network	Q, AE, AP, AW, BH	-	34
50	DSMAP [25]	ECCV	2020	Github	Domain-specific Content Mappings	AQ, AW, AX	-	13
51	ACL-GAN [79]	ECCV	2020	Github	Adversarial Consistency Loss, MUNIT	I, AU	-	29
52	DRIT++ [27]	IJCV	2020	Github	Disentangled Representation with Cross-cycle Consistency	AP, AQ, AW, AX, I	-	218
53	CoCosNetv2 [82]	CVPR	2021	Github	ConvGRU Module, Hierarchical Strategy, PatchMatch	AE	-	32
54	SofGAN [83]	TOG	2022	Project	SOF Net, StyleGAN, Style Mixing, SPADE	AC, BU, I	Bm., Sm., Attri.	11

Table 3 Summary of popular related works. Please refer to Table 2 for more detailed descriptions.

#	Model	Publ.	Year	Code	Component	Dataset	Assist.	Cite.
Deep Image-to-Sketch Synthesis								
55	FCRL [126]	ICMR	2015	-	Fully Convolutional Network	Y	-	127
56	DGFL [127]	IJCAI	2017	-	Deep CNNs, Graphic model	Y	-	34
57	Scribbler [128]	CVPR	2017	Project	Encoder-decoder with residual connections, GAN	Y, E	-	427
58	FSSC2F [129]	AAAI	2018	-	U-Net, Probabilistic Graphic Model	Y	-	11
59	TextureGAN [130]	CVPR	2018	Github	Local Texture Loss, VGG Loss, Scribbler	E, S	Bm. Tp.	221
60	SCC-GAN [131]	CVPR	2018	Code	Hybrid model, Shortcut Cycle Consistency	AK, AL	-	76
61	ContextualGAN [132]	ECCV	2018	Github	Contextual Loss, Joint Representation, GAN	I, Z, CB	-	74
62	pGAN [133]	IJCAI	2018	Github	UNet, Parametric Sigmoid, CycleGAN	Y, CU	Bm.	24
63	MRNF [134]	IJCAI	2018	-	Markov Random Neural Fields	Y	-	16
64	PSS [~] 2S-MAN [135]	FG	2018	Github	Multi-Adversarial Networks, CycleGAN	Y, CU	-	98
65	DualT [136]	TIP	2018	-	Deep Features, Intra- and Inter-Domain Transfer	Y	-	51
66	MDAL [11]	TNNLS	2018	Github	Domain alignment, Interpreting by Reconstruction	Y, CU	-	45
67	FAG-GAN [137]	WACVW	2018	-	Attribute Classification, Conditional CycleGAN	I, C	-	30
68	Geo-GAN [138]	BIOSIG	2018	Github	Geometry Discriminator, CycleGAN	CU, C	-	17
69	PI-REC [139]	arXiv	2019	Github	Corse-to-Fine, LSGAN, VGG Loss	A, I, S, AT	Cm.	18
70	DLLRR [140]	TNNLS	2019	-	Coupled Autoencoder, Low-rank Representation	Y	-	27
71	Col-cGAN [141]	TNNLS	2019	-	Collaborative Loss, cGAN, Deep Collaborative Nets	Y, CU	-	43
72	CFSS [142]	TIP	2019	-	cGAN, VGG, Feature Selection	Y	-	14
73	KT [143]	IJCAI	2019	-	Knowledge Transfer, Teacher-Student Net	Y, CU	-	16
74	im2pencil [144]	CVPR	2019	Github	Outline and Shading Branch Networks, Pix2pix	E	Sv.	28
75	ISF [145]	ICCV	2019	Project	Shape and Appearance Generators, Two-stage	S, AC, E	-	62
76	APDrawing [2]	CVPR	2019	Github	Hierarchical GAN, DT Loss, Local Transfer Loss	AS	Fl., Bm., Sv.	82
77	APDrawing++ [10]	TPAMI	2020	Github	APDrawing, Line Continuity Loss	AS	Fl., Bm., Sv.	12
78	UPDG [9]	CVPR	2020	Github	Asymmetric CycleGAN, Cycle-consistency Loss	BJ	Fl., Bm., Sv.	22
79	WCR-GAN [146]	CVPR	2020	Github	Cartoon Representation Learning, GAN	F, BU, BV, E	-	29
80	EdgeGAN [147]	CVPR	2020	Project	SketchyCOCO, Divide-and-Conquer strategy	F	Attri.	34
81	DeepPS [148]	ECCV	2020	Github	Sketch Refinement with Dilations, Pix2pixHD	AC, I	-	25
82	DeepFaceDrawing [149]	TOG	2020	Github	Component Embedding, Feature Mapping, Image Synthesis	AC, E	Km.	41
83	CA-GAN [150]	TC	2020	Github	Composition/Appearance Encoder, P-Net, Stacked GAN	Y, CU	Fl.	44
84	IDA-CycleGAN [151]	PR	2020	-	CycleGAN, Identity Loss, Recognition Model	Y, CU	-	41
85	IPAM-GAN [152]	SPL	2020	-	Identity-preserved Adversarial Model, U-Net	Y, CU	-	12
86	MvDT [153]	TIP	2020	Github	CNN [89] Features, Hand-crafted Features	Y, E	-	10
87	MSG-SARL [154]	TIFS	2021	-	Self-attention Residual Learning, Multi-scale Gradients	Y, CU	-	6
88	GANSketching [155]	ICCV	2021	Project	Weight Adjusting, Cross-domain Fine-tuning	CH, AL	-	8
89	DoodleFormer [156]	Arxiv	2021	-	Transformer, Part Locator and Part Sketcher Networks	CK	-	1

the universal style transfer. Similar to I2SGAN [91], Richardson *et al.* [86] improved the classical StyleGAN with a novel encoder network that learns many style vectors that are fed into a pre-trained generator, forming an extended \mathcal{W} -latent space.

2.4 Deep Photo-Sketch Synthesis

Deep photo-sketch synthesis is a recent branch of the FSS task, in which deep learning is used to improve performance and quality. The related works can be divided into three categories. The first aims to translate any sketch images into their corresponding RGB images. The second tries to convert any RGB images into sketch images. The last mainly focuses on facial-sketch synthesis.

General S2I. Xian *et al.* [130] proposed the TextureGAN model to synthesize an image under the supervision of a sketch, color, and texture. TextureGAN consists of a ground-truth pre-training module and an external texture fine-tuning part. Then, Lu [132] *et al.* introduced a two-stage contextual GAN to achieve sketch-to-image generation. This framework trains a classical GAN model with a newly

defined loss, representing the joint distribution and capturing the inherent relation between a sketch and its corresponding image. Inspired by image in-painting [157], You *et al.* [139] proposed the PI-REC model, which contains three phases: an imitation phase, generating phase, and refinement phase. PI-REC is progressively trained using only one generator and one discriminator. The ISF introduced in [145] is a gating-based approach, which allows a single generator to be used to generate distinct classes without feature mixing. Recently, Gao *et al.* [147] proposed EdgeGAN for object-level image synchronization given freehand scene sketches. This framework contains two sequential modules: foreground generation and background generation. Yang *et al.* [148] presented a deep plastic surgery model to simulate the coarse-to-fine painting process of human artists. Chen *et al.* [149] proposed a local-to-global framework to allow any user to produce high-quality face images. Their model consists of three modules: component embedding, feature mapping, and image synthesis.

General I2S. Song *et al.* [131] proposed the first deep stroke-level photo-to-sketch synthesis method, which is a hybrid model with a shortcut

cycle consistency constrained by a VAE-style reconstruction loss. As the default settings of I2I and NST, both can synthesize artistic portrait drawing (APD) images. However, they do not meet practical requirements because APD images usually have a highly abstract style and graphic elements. Therefore, Yi *et al.* [2] proposed APDrawing to transform an input face image into its corresponding APD image, in which a hierarchical GAN model is built by combining both a global and a local network. Then, they further proposed an APDrawing++ [10], in which they used an auto-encoder to refine subtle facial features and presented a novel line continuity loss to enhance the line continuity of APDrawing. However, both of these APDrawing methods require pair-wise data for training. To handle this problem, Yi *et al.* thus proposed an asymmetric cycle-structure GAN [9], which contains a relaxed forward cycle consistency loss (*a.k.a.* truncation loss) to prevent the reconstructed photo from being noisy, and a strict cycle consistency loss to enhance the performance. This method also uses multiple local discriminators to ensure the quality of the facial portrait drawings. Different from portrait drawing, Wang *et al.* [146] observed the behavior and properties of cartoon paintings and proposed three different representations considering surface, texture, and shape information, respectively. In addition, they also released the new SketchyCOCO dataset to better train and evaluate the performance of their model. Based on Pix2pix, Li *et al.* [144] designed a two-branch network (called im2Pencil) to implement photo-pencil translation, which can simulate sketch outlines and shadows. Wang *et al.* [155] presented a GAN sketching method to rewrite a GAN with one or more sketches. This new method uses regularizations to preserve the original GAN's diversity and image quality while matching the generated sketch images with users' needs through a cross-domain adversarial loss. Bhunia *et al.* [156] introduced a new transformer architecture to generate various yet realistic creative sketches consisting of two networks. The first part of locator networks aims to capture the coarse structure by observing the relationship between local patterns. The second part of the sketcher network, follows the standard GAN, which aims to synthesize high-quality sketches.

Photo-Sketch Synthesis. Zhang *et al.* [126] were the first to use a fully convolutional neural network (FCNN) to build a deep photo-to-sketch synthesis model. Then, the works [103, 129, 134] integrated deep features into probabilistic graph model learning, achieving better performance than traditional models [1, 50]. To make the network more flexible, Zhang *et al.* [133] took the key idea of CycleGAN and proposed a novel pGAN, which uses a special parametric Sigmoid activation function to reduce the effects of photo priors and illumination variations. To improve the quality of generated photo/sketch, Wang *et al.* [135] introduced a synthesis method using multi-adversarial networks (PS²MAN). Their model uses two U-Nets to generate high-quality images from low to high resolution. To achieve the same goal, Zhang *et al.* [11] further proposed a facial-sketch synthesis by multi-domain adversarial learning (MDAL), which overcomes the defects of blur and deformation. The basic idea behind MDAL is the concept of “interpretation through synthesis”, which is built upon two diverse generators. Kazemi *et al.* [137, 138] proposed an improved version of CycleGAN, which focuses on the facial attributes during the portrait synthesis process. Zhang *et al.* [140, 142] introduced two methods by combining an auto-encoder and traditional subspace learning, which is more effective than the traditional FSS methods. Besides, Zhu *et al.* [141] proposed a collaborative framework that exploits the interaction information of two opposite generators by introducing a collaborative loss. However, it is difficult to train a good model due to the lack of large-scale training data. Therefore, Zhu *et al.* [143] proposed using classical knowledge distillation to learn two well-defined student mapping networks via two strong teacher networks. More recently, the works in [151, 152] introduced identity-aware models, which use a new perceptual loss to train a better image generative model, and thus consider the downstream task, *e.g.*, face recognition, as the final goal. Yu *et al.* [150] proposed a new composition-assisted generative adversarial network, which helps synthesize realistic facial sketches/photos by using facial composition information. By leveraging the relationships between features, [154] implemented a multi-scale self-attention residual learning framework for face

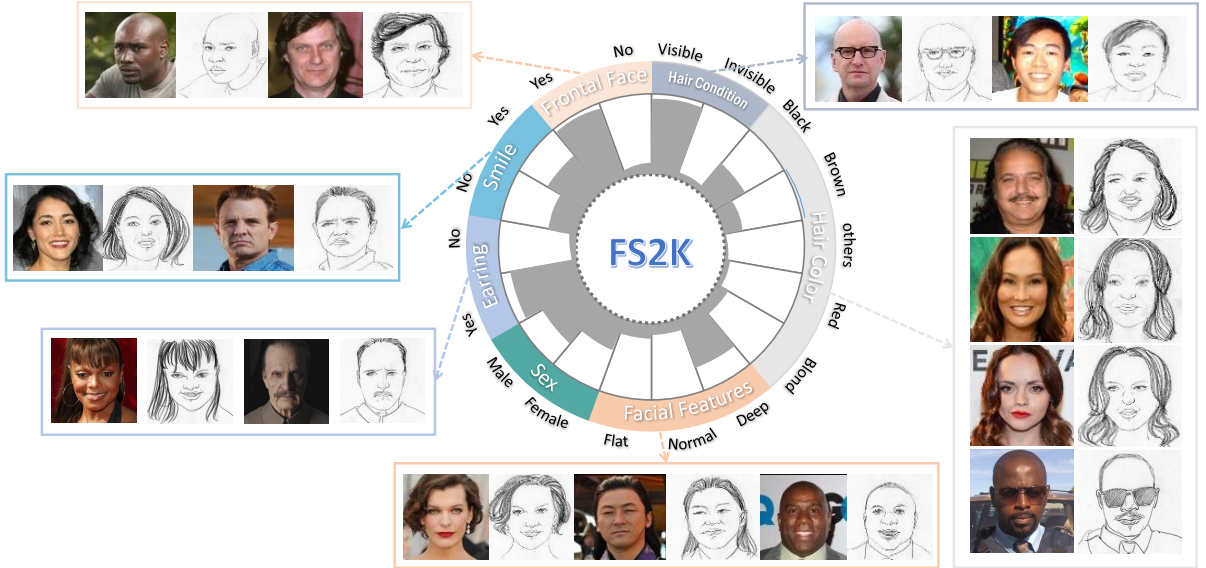


Fig. 4 Statistics and examples from the FS2K dataset. Please refer to Sec. 3 for details.

photo-sketch conversions. Finally, the method proposed in [153] does not need any images from the source domain for training, enabling it to leverage both deep features (extracted from the CNN) and handcrafted features flexibly.

3 Proposed FS2K Dataset

In this section, we introduce the proposed FS2K. Some example images are shown in Fig. 2. We describe FS2K in terms of two key aspects, namely dataset collection, and data annotation. Overall, FS2K includes 2,104 photo-sketch pairs, which are split into 1,058 for training and 1,046 for testing. The complete dataset is available at <https://github.com/DengPingFan/FS2K>.

3.1 Data Collection

To establish a long-lasting benchmark, the data should be carefully selected to cover diverse scenes from different views, such as lighting conditions, skin colors, sketch styles, and image backgrounds. To this end, we introduce FS2K, a new high-quality dataset⁵ for the FSS task.

Our FS2K includes 2,104 photos from real scenes, the Internet, and other datasets. The majority, however, come from

CASIA-WebFace [158], which is a large-scale (*i.e.*, 500K images) labelled dataset of faces in the wild. CASIA-WebFace was collected from the IMDb⁶ website and contained well-organized information, such as name, gender, and birthday. Thanks to the rich and clean open-source data from CASIA-WebFace, it could be used to build our high-quality and representative benchmark. We manually selected 1,529 images to cover a large span of major challenges faced in realistic scenes, such as varying background, hairstyle (*e.g.*, long, short), accessories (*e.g.*, glasses, earrings), and skin information (*e.g.*, patch image on a given face). Because the photos selected in CASIA-WebFace are taken from a single angle, multi-angle face images for the same person are missing. To this end, we invited eight actors to take 98 photos under different settings (*e.g.*, lighting conditions, face angles). In addition, to further increase the diversity, we also collected some children’s photos and some faces with smaller face-to-image ratios. The remaining 477 face photos come from other free stock photo websites, including Unsplash,⁷ Pexels,⁸ Pngimg,⁹ and Google.

⁶<http://www.imdb.com>

⁷<http://www.unsplash.com>

⁸<http://www.pexels.com/>

⁹<http://pngimg.com/>

⁵This dataset is for scholarly communication only.

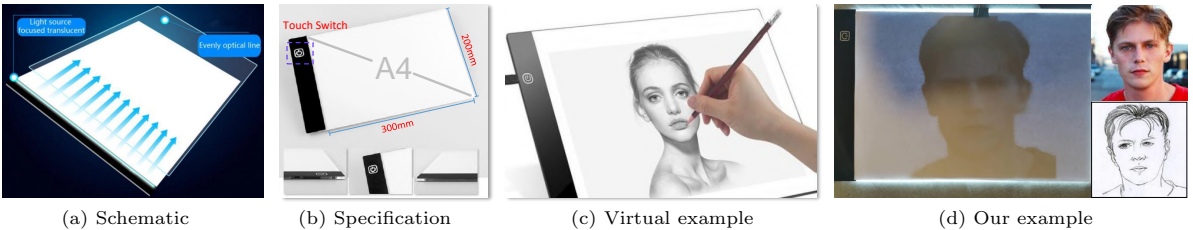


Fig. 5 Use of the copy table and an example. Zoomed-in for the best view. See Sec. 3.2 for more details.

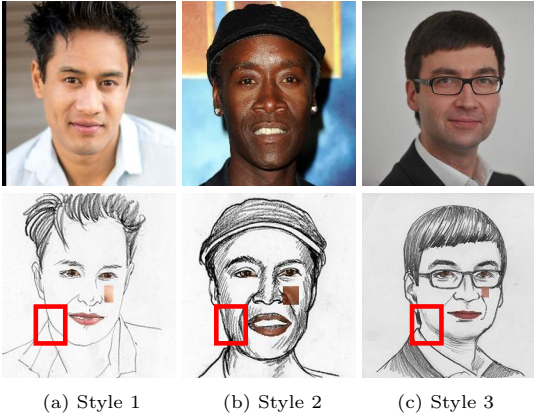


Fig. 6 Three sketch styles in our FS2K. As shown in the cheek region, the styles include simple lines (style 1), long strokes (style 2) and repeated wispy details (style 3).

3.2 Data Annotation

There are four types of annotations in our FS2K, including sketch drawing, sketch style, color, and contour feature annotations.

3.2.1 Sketch Drawing

Participants. Three senior artists (including two male and one female) from the Sichuan Fine Arts Institute were hired to participate in the study.¹⁰ All three participants had normal or corrected to normal vision. None of the participants suffered color-blindness or color-weakness. The participants ranged in age from 20 to 23 years, with an average of five years of professional experience in sketch drawing.

Apparatus. The three artists drew all sketch images with the assistance of a Copy Table LED Board.¹¹ Fig. 5 shows the copy table we used and

¹⁰The <https://www.scfai.edu.cn/english/> is one of the four most prominent art academies in China. The three senior artists are all from the Design Academy.

¹¹Fig. 5-a presents the copy table, which has an LCD backlight. It requires a high voltage input of 100 ~ 240V and 0.6A working current. Its size is A4 (*i.e.*, 300 × 200 ×

an example (Fig. 5-d) of a face sketch drawn by our artists. The touch switch region in our device supports three levels of adjustable brightness, so the artists can use the button to change the brightness they desire. This helped them locate the contours of facial features according to the photo information from the bottom of the LED board. Moreover, this equipment also helped to ensure content similarity and face alignment between sketches and corresponding photos. At the same time, the drawings retain the artist's sketch style.

3.2.2 Sketch Style Annotation

Our FS2K contains three different styles, which enrich the diversity of sketches, as shown in Fig. 6. This enables different artists' skills to be captured while making FS2K more challenging than previous FSS datasets.

We created a balanced dataset to facilitate the comparison of different methods, *i.e.*, the number of the images with the three different styles are equally distributed. Specifically, in the training set, the samples with style1, style2, and style3 are 357, 351, and 350, respectively. In the test set, they are 619, 381, and 46, respectively.

3.2.3 Facial Feature Annotation

Sketches are rapidly executed freehand drawings, which have less attribute information than the original images, *e.g.*, facial texture, facial expressions [159], and facial posture. Therefore, it is challenging to restore real images (*i.e.*, S2I task) based on a single sketch image. Meanwhile, in real-world applications, we can use auxiliary facial information (such as gender, accessories, and

3.5mm) in Fig. 5-b, and the luminous intensity is 300 ~ 350LM. Therefore, it has become the most popular copy table product, after the aluminum alloy copy table, for animators (see Fig. 5-c).

Table 4 Number of images for each attribute in the training and test datasets.

FS2K (Ours)	w/ H	w/o H	H(b)	H(bl)	H(r)	H(g)	M	F	w/ E	w/o E	w/ S	w/o S	w/ F	w/o F	S1	S2	S3
Train	1010	48	288	423	60	239	574	484	209	849	645	413	917	141	357	351	350
Test	994	52	290	418	44	242	632	414	187	859	670	376	872	174	619	381	46

hairstyle) to narrow down a suspect in a database. Following [160], we added some additional facial feature annotations, including *gender*, *smile*, *face pose*, *hair condition*, *hair color*, *earring*, and *skin texture*. We hired two data annotators to label all photos and performed cross-checking to ensure the accuracy of the final annotations. Overall labels can be found in Table 4, while the details of each are described below.

Gender. Gender is a high-level human attribute commonly used in traditional face databases such as CelebA [28] and LFW [161]. It has been extensively studied in face detection and recognition [162–164]. Therefore, we carefully labelled all photos in FS2K with gender attributes. Specifically, there were 574 male photos and 484 female photos in the training set, and 632 male photos and 414 female photos in the test set.

Smile. Smiling is a primary human activity that represents a positive emotional state. As such, many studies have focused on smile detection [165, 166] or used smile as an attribute for recognition [167]. Therefore, we also consider a smile a key attribute in our dataset. Specifically, the training set contains 645 smiling people and 413 with no obvious expression, while the test set contains 670 smiling people and 376 with no expression. We ensured that the proportion of smiling people in the training and test sets was as close as possible.

Face Pose. The facial attributes may cover only a small part of the image, but the photo is usually dominated by the effects of pose [168]. Moreover, pose will affect the performance of face recognition [169], tracking [170], and synthesis [171]. Therefore, the facial pose is useful auxiliary information. We define a portrait with the head rotated within 30 degrees as a frontal face pose. According to this definition, the training set has 917 frontal photos, while the test set has 872. The remaining have side face poses.

Hair Status and Color. Hair is a saliency feature of the head that may change in different situations. Even if there is sufficient information in the internal features of the face for recognition, manipulating the hair can harm the performance

[172, 173]. Moreover, facial synthesis and retrieval systems often use hair as an important cue [174, 175] to improve the quality of generated images. For FSS, although the sketches contain the hair contour, the corresponding color information and hair status (with or without hair) are missing. Therefore, in FS2K, we provide annotations of the hair status, which includes four available colors (*i.e.*, black, brown, red, and blond) and another status (*i.e.*, bald or wearing a hat), as shown in Fig. 4. In other words, for faces with hair, we mark the color information directly, while cases of thinning hair or wearing a hat are marked as separate attributes. The statistical results of this annotation can be found in Table 4.

Earrings. The simplified characteristics of sketch drawings lead to unclear earring contours. Meanwhile, as shown in Fig. 4, earrings in real photos are visible. Therefore, in FS2K, we provide annotations for whether earrings are present, which can help the model training. Specifically, the training set has 209 people with earrings, and the test set has 187.

Skin Texture. Skin texture provides a large amount of detailed local information and is used as a vital feature for face recognition [176, 177]. However, this critical information is completely lost in sketch images. Therefore, we clip a small patch from the real photo and use it as the skin texture, as shown in Fig. 6. We also include the average RGB value for the corresponding lip and eyeball region to provide more information for future research.

4 Proposed FSGAN Baseline

4.1 Problem Definition

Facial synthesis (FS) aims to generate target representations of human faces based on the given inputs. This process can be formulated as $X_o = F(X_i)$, where X_i and X_o denote the input and output (*e.g.*, RGB images and sketches) of facial representations F indicates the synthesis function. In this paper, based on the overall architecture of [2, 10], we design the

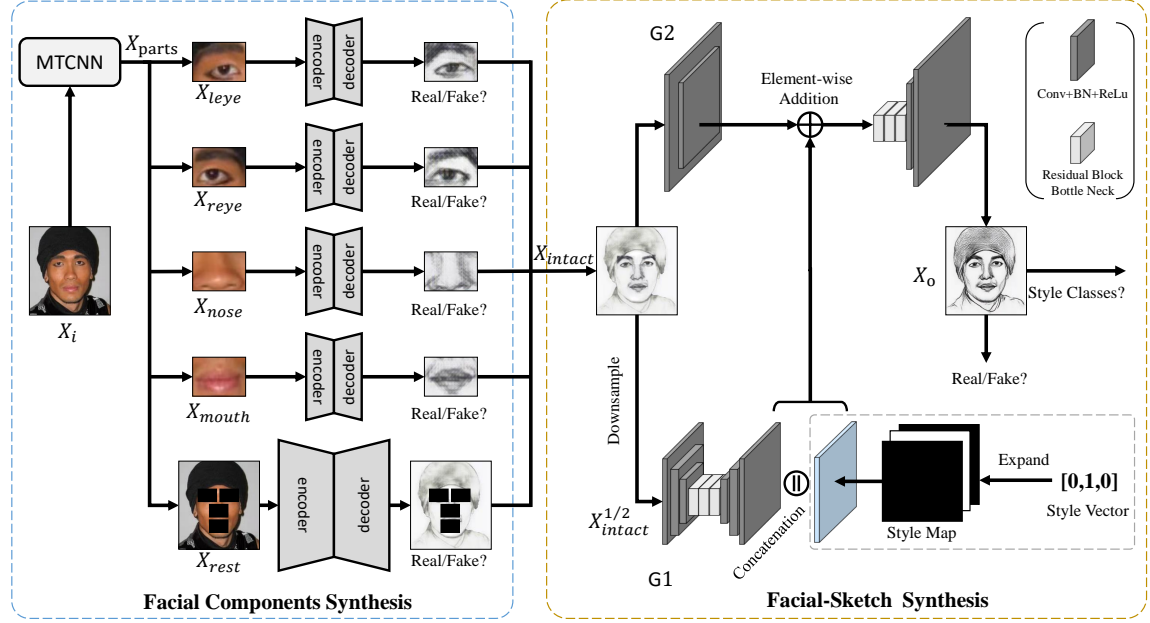


Fig. 7 Pipeline of our FSGAN baseline for the I2S task. It consists of two stages: 1) facial components synthesis and 2) facial-sketch synthesis. Please refer to Sec. 4.2 and Sec. 4.3 for more details.

baseline, FSGAN, for both the I2S task¹² and S2I task,¹³ inspired by pix2pixHD [23]. Instead of focusing on direct image-level facial synthesis, we propose a two-stage “bottom-up” facial synthesis architecture, as shown in Fig. 7. Hence, our FSGAN consists of two cascaded stages built upon multiple generative models (*i.e.*, GANs).

The first stage comprises of five parallel GANs, which are designed to synthesize the local facial components separately. Given an input, four facial regions (*e.g.*, left eye, right eye, nose, and mouth) and the rest of the inputs are cropped and fed into their corresponding GANs in the first stage to synthesize key facial features. These synthesized facial component patches are then stitched together to obtain the intact facial representation. Since the local facial patches are synthesized independently, the connecting region of the stitching, as well as their appearances, are inconsistent with each other. Therefore, the second stage is introduced to further refine the results by considering the global structure and texture. In this stage, the style vectors of the facial sketches are utilized to assist the synthesis.

¹² $X_{ske} = F(X_{img}, X_{style})$, where X_{style} denotes the sketch style of input.

¹³ $X_{img} = F(X_{ske})$.

4.2 Facial Components Synthesis

Almost all human faces have the same global structure. The differences lie in the details of the local facial components, such as eyes, eyebrows, nose, and mouth. To capture more details of different facial components, the first stage of our model synthesizes them separately. Specifically, given a facial input, the four key patterns, including the left eye, right eye, nose, and mouth, are first detected by MTCNN [178]. The input X_i is then divided into five parts, $X_{parts} = \{X_{leye}, X_{reye}, X_{nose}, X_{mouth}, X_{rest}\}$, based on the detection results. These include the left eye, right eye, nose, mouth, and remaining components. Five parallel GANs are utilized to synthesize their corresponding patches for these parts. Therefore, the problem can be formulated as $G_{parts} = \{G_{leye}, G_{reye}, G_{nose}, G_{mouth}, G_{rest}\}$ and $D_{parts} = \{D_{leye}, D_{reye}, D_{nose}, D_{mouth}, D_{rest}\}$, where G and D indicate the generator and discriminator, respectively.

First, the four GANs synthesizing the left eye, right eye, nose, and mouth have the same architecture. Each GAN consists of a generator and a discriminator. The generator is designed as an encoder-decoder, consisting of an encoder, a bottom connection, and a decoder. The encoder

is composed of three convolutional blocks, each of which is a combination of a convolutional layer (with a kernel size of 3 and stride of 2), a batch normalization layer, and a ReLU activation layer. Meanwhile, the second bottom connection consists of nine bottleneck residual blocks that are similar to [179]. Finally, the decoder is built upon three deconvolutional blocks: a deconvolutional layer, a batch normalization layer, and a ReLU activation layer. Note that the GAN, which is used for synthesizing X_{rest} , is similar to the previously described ones. However, the encoder contains four convolutional blocks, and the decoder comprises four deconvolutional blocks to achieve larger receptive fields.

The discriminators of the above five GANs are the same. Each consists of three cascaded convolutional layers (with a kernel size of 3 and stride of 2) followed by global average pooling. Then, a 1×1 convolutional layer and a sigmoid function are used to predict the probability of the generated results being real or fake.

Based on the above design, the first stage of FSGAN can restore details of the facial components in both the I2S and S2I tasks. At the end of this stage, the synthesized patches are stitched together to restore the intact facial synthesis result X_{intact} . Since different generators synthesize the patches, their overall appearances are inconsistent, which becomes even more obvious in the stitched result. To this end, the stitched result is then fed to the next stage to adjust and refine the global structure and appearance.

4.3 Facial-Sketch Synthesis

To address the inconsistency issue of the output from the first stage, we introduce the second stage, which is designed as another GAN model inspired by Pix2pixHD [23], for local detail refinement and global structure adjustment.

In this stage, we use the multi-scale discriminators D_{fs} and the coarse-to-fine generator G_{fs} following Pix2pixHD [23]. Specifically, the generator G_{fs} consists of two sub-networks $G1$ and $G2$, both of which follow encoder-decoder architecture, as shown on the right part of Fig. 7. We sample the output of the first stage using a downsampling operation with a sampling rate of 50%. This newly sampled

image $X_{intact}^{1/2}$ ($height/2, width/2$) is then fed into the first sub-network $G1$, which is designed to capture global features. The other sub-network $G2$ is employed to capture the local details, which takes the output of the first stage as input. We use both concatenation and element-wise addition operations to fuse the style, local, and global information. Specifically, the concatenation combines the style feature map and the output of $G1$ and generates a new fused feature map. Then, the element-wise addition is utilized to combine this new feature map with the latent feature of the encoder part of $G2$. Finally, we use the decoder part of $G2$ to generate the final output X_o . It is worth noting that the style vector can control the style of the generated sketches, which helps improve their quality and diversity. Besides, the style of the real photo is often fixed, and independent from the artists' style. Therefore, we introduce the style information in the I2S task but exclude that in the S2I task.

4.4 Loss Function

We use a combination of several loss functions to train our model. We denote X and Y as the input and its corresponding reference, respectively. For simplicity, we define $G(X)$ as the generated output of the given input X and $D_k(X, Y)$ as the corresponding predicted probabilities of the k -th discriminator. Then, we denote the i -th layer feature extractor of discriminator D_k as D_k^i , where k is the index of the discriminator.

Adversarial Loss. We use the adversarial loss [73] to make the generated image more visually appealing. The adversarial loss we use is defined as:

$$L_{\text{adv}}(G, D) = \mathbb{E}_{X, Y}[\log D(X, Y)] + \mathbb{E}_X[1 - \log D(X, G(X))]. \quad (1)$$

Feature Matching Loss. Similar to [23], we use the feature matching loss to improve the adversarial loss based on the k -th discriminator. The feature matching loss is defined as:

$$L_{\text{fm}}(G, D_k) = \mathbb{E}_{X, Y} \sum_{i=0}^T \frac{1}{N_i} [\|D_k^i(X, Y) - D_k^i(X, G(X))\|_1], \quad (2)$$

where T denotes the total number of layers in each discriminator and N_i is the number of feature

maps in the i -th layer. This loss is used to match the intermediate feature maps of the real and synthesized images, making the generator produce multi-scale statistical information. Besides, it stabilizes the training process and restores highly realistic outputs.

Perceptual Loss. To maintain perceptual and semantic consistency, we use a perceptual loss [93] to measure the difference between the original image and the corresponding synthesized image. We extract the perceptual features from the i -th layer activations of a pre-trained VGGNet [89], which is denoted as $\phi_i(\cdot)$. The perceptual loss is defined as follows:

$$L_{\text{per}}(G(X), Y) = \mathbb{E}_{G(X), Y} \sum_{i=0}^t \|\phi_i(Y) - \phi_i(G(X))\|_1. \quad (3)$$

Pixel-Wise Loss. The L_1 distance between a generated image $G(X)$ and reference Y is regarded as the pixel-wise loss, which is defined as:

$$L_1(G(X), Y) = \frac{1}{h \times w} \sum_{(i,j)=(0,0)}^{(h,w)} \|Y(i, j) - G(X)_{(i,j)}\|_1, \quad (4)$$

where (i, j) and (h, w) are the pixel coordinates and the (height, width) of the output, respectively.

Style Classification Loss. Similar to [180, 181], we define an auxiliary classifier to predict the sketch style of the generated image. For any generated image $G(X)$, the style classification loss is defined as:

$$L_{\text{sty}}(G, S, c) = \mathbb{E}_{X, c} [l_{\text{ce}}(S(G(X)), c)], \quad (5)$$

where $l_{\text{ce}}(\cdot, \cdot)$ is the cross-entropy loss, $S(\cdot)$ is a CNN that outputs the probability over different styles, and c is the label of a given artist's style. Note that we only use the style classification loss in the second stage for the I2S task.

Overall Loss. Finally, the overall loss function for the multi-scale discriminators is:

$$L_{D \sim (D_{\text{parts}}, D_{\text{fs}})} = \sum_i^K -L_{\text{adv}} + \lambda_{\text{fm}} L_{\text{fm}}, \quad (6)$$

and the overall loss function for generator is:

$$\begin{aligned} & L_{G \sim (G_{\text{parts}}, G_{\text{fs}})} \\ &= L_{\text{adv}} + \lambda_{\text{fm}} L_{\text{fm}} + \lambda_1 L_1 + \lambda_{\text{per}} L_{\text{per}} + \lambda_{\text{sty}} L_{\text{sty}}, \end{aligned} \quad (7)$$

where λ_{fm} , λ_1 , λ_{per} , and λ_{sty} are hyperparameters that control the importance of the feature matching loss, pixel-wise loss, perceptual loss, and style classification loss, respectively.

4.5 Implementation Details

We use PyTorch [182] to implement the baseline FSGAN. The experiments are conducted on an NVIDIA V100S.

For the I2S task, we set $\lambda_{\text{fm}} = 25.0$, $\lambda_1 = 25.0$, and $\lambda_{\text{per}} = 12.5$ to train the model in the facial components synthesis stage, and set $\lambda_{\text{fm}} = 100.0$, $\lambda_1 = 100.0$, $\lambda_{\text{per}} = 50.0$, and $\lambda_{\text{sty}} = 100.0$ for facial synthesis. The Adam optimizer [183] is used for training the whole network. The initial learning rates for the generator and discriminator are $2e-4$ and $1e-5$, respectively. The other hyperparameters of the optimizer are set to the default values as recommended in PyTorch. We set the number of epochs to 50. All generators and discriminators are trained iteratively.

For the S2I task, we set $\lambda_{\text{fm}} = 50.0$, $\lambda_1 = 50.0$, and $\lambda_{\text{per}} = 0.2$ to train the neural network for the facial component synthesis stage, and set $\lambda_{\text{fm}} = 100.0$, $\lambda_1 = 100.0$, and $\lambda_{\text{per}} = 0.2$ for facial synchronization. We again use the Adam optimizer, with initial learning rates of $2e-4$ for both the generators and discriminators. The training strategy is almost the same as that for the I2S task. However, we set the number of epochs to 400,¹⁴ freezing the weights of the facial components synthesis module after 250 epochs and further training the facial synthesis module for the remaining epochs.

5 Benchmark

This section provides comprehensive comparisons and analyses of the existing models on FS2K, in terms of both the I2S and S2I tasks.

¹⁴Because the S2I task needs to restore more detailed information of the RGB images, more training epochs are needed.

Table 5 Quantitative results of popular models on the I2S task. “↑” means the higher, the better. Publ.: Publication information.

#	Model	Publ.	SCOOT↑	SSIM↑
1	DualGAN [78]	Yi <i>et al.</i> ICCV	0.261	0.324
2	FPST [95]	Chen <i>et al.</i> NeurIPS	0.271	0.460
3	NST [87, 88]	Gatys <i>et al.</i> CVPR	0.273	0.326
4	Pix2pix [31]	Isola <i>et al.</i> CVPR	0.275	0.438
5	ACL-GAN [79]	Zhao <i>et al.</i> ECCV	0.278	0.404
6	WCT [124]	Li <i>et al.</i> NeurIPS	0.282	0.369
7	AdaIN [123]	Huang <i>et al.</i> ICCV	0.303	0.365
8	UNIT [22]	Liu <i>et al.</i> NeurIPS	0.304	0.504
9	TSIT [80]	Jiang <i>et al.</i> ECCV	0.307	0.441
10	DRIT++ [27]	Lee <i>et al.</i> IJCV	0.308	0.492
11	CartoonGAN [85]	Chen <i>et al.</i> CVPR	0.319	0.400
12	UGATIT [30]	Kim <i>et al.</i> ICLR	0.323	0.457
13	NICE-GAN [26]	Chen <i>et al.</i> CVPR	0.327	0.473
14	CycleGAN [21]	Zhu <i>et al.</i> ICCV	0.348	0.435
15	MDAL [11]	Zhang <i>et al.</i> TNNLS	0.355	0.466
16	UPDG [9]	Yi <i>et al.</i> CVPR	0.364	0.471
17	Pix2pixHD [23]	Wang <i>et al.</i> CVPR	0.374	0.492
18	APDrawing [2]	Yi <i>et al.</i> CVPR	0.375	0.464
19	DSMAP [25]	Chang <i>et al.</i> ECCV	0.378	0.493
20	FSGAN	Fan <i>et al.</i> MIR	0.405	0.510

5.1 Experimental Settings

5.1.1 Evaluation Metrics

For the I2S task, the most popular facial sketch metric is the structural similarity index metric (SSIM) [20, 44]. However, it ignores the perceptual similarity between a prediction and the reference. Therefore, we further adopt the recently proposed structure co-occurrence texture (SCOOT) metric [29], which provides a unified evaluation for both structure and texture. For the S2I task, we still adopt the widely used SSIM metric to evaluate the synthesized faces. Our evaluation toolbox is available at <https://github.com/DengPingFan/FS2KToolbox>.

5.1.2 Comparison of the Models

To evaluate the performance on the I2S task and S2I task, we present the empirical results of 19 representative approaches and the FSGAN baseline.

5.1.3 Training/Testing Protocols

All compared methods are selected on three criteria: a) widely regarded technology, b) open-source code, and c) state-of-the-art performance. The models are trained and tested on our FS2K with the image sizes specified in their papers. If the size setting is not provided in their paper, 512×512 is utilized as the default.

5.2 Overall Results and Analysis

5.2.1 I2S Task

We first provide a performance summary of the I2S task regarding both SCOOT and SSIM scores. Quantitative results and qualitative comparisons are shown in Table 5 and Fig. 8–10, respectively. The experimental observations indicate that the FSGAN baseline achieves better results. For further analysis, we divide all compared methods into three categories based on their SCOOT score:

- score ≤ 0.3 ;
- $0.3 < \text{score} \leq 0.35$;
- $0.35 < \text{score}$.

Analysis. Methods in the first group achieve a SCOOT below 0.3. These include DualGAN [78], FPST [95], NST [87, 88], Pix2pix [31], ACL-GAN [79], and WCT [124]. As shown in Fig. 8, DualGAN, NST, and WCT suffer from structural distortion, where many local facial details are lost. The images produced by the DualGAN are poor, and it is challenging to detect facial components in them. This explains why it has lower SSIM and SCOOT scores. In addition, compared with other results, Pix2pix and FPST generate blurred results. ACL-GAN seems to achieve satisfactory results in visual appeal, yielding a higher SSIM score. However, ACL-GAN reproduces the original facial structure almost exactly, lacking artistic style.

The second group includes AdaIN [123], UNIT [22], TSIT [80], DRIT++ [27],

Table 6 Quantitative results of popular models on the S2I task. “↑” means the higher, the better.

#	Model	Publication	SSIM↑
1	DualGAN [78]	Yi <i>et al.</i> ICCV	0.241
2	WCT [124]	Li <i>et al.</i> NeurIPS	0.311
3	ACL-GAN [79]	Zhao <i>et al.</i> ECCV	0.314
4	TSIT [80]	Jiang <i>et al.</i> ECCV	0.316
5	UGATIT [30]	Kim <i>et al.</i> ICLR	0.317
6	NST [87, 88]	Gatys <i>et al.</i> CVPR	0.335
7	CycleGAN [21]	Zhu <i>et al.</i> ICCV	0.339
8	Pix2pix [31]	Isola <i>et al.</i> CVPR	0.346
9	SPADE [24]	Park <i>et al.</i> CVPR	0.361
10	UNIT [22]	Liu <i>et al.</i> NeurIPS	0.362
11	AdaIN [123]	Huang <i>et al.</i> ICCV	0.373
12	DRIT++ [27]	Lee <i>et al.</i> IJCV	0.381
13	FNS [93]	Johnson <i>et al.</i> ECCV	0.391
14	NICE-GAN [26]	Chen <i>et al.</i> CVPR	0.397
15	FPST [95]	Chen <i>et al.</i> NeurIPS	0.400
16	pSp [86]	Richardson <i>et al.</i> CVPR	0.428
17	Pix2pixHD [23]	Wang <i>et al.</i> CVPR	0.433
18	DSMAP [25]	Chang <i>et al.</i> ECCV	0.471
19	DeepPS [148]	Yang <i>et al.</i> ECCV	0.487
20	FSGAN	Fan <i>et al.</i> MIR	0.503

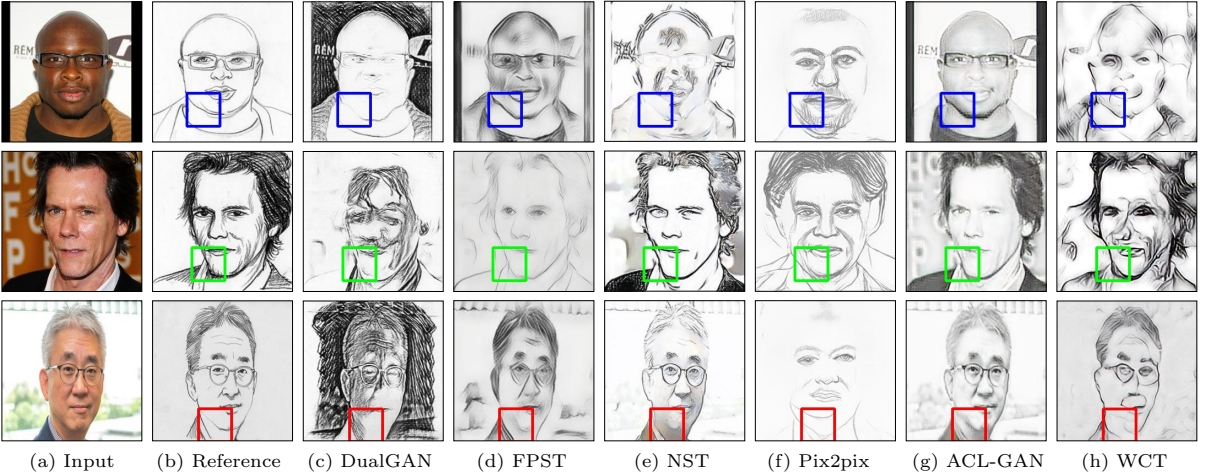


Fig. 8 From left to right: input face, reference, DualGAN [78], FPST [95], NST [87, 88], Pix2pix [31], ACL-GAN [79], and WCT [124]. We mark the three styles with blue, green, and red boxes for each result. Zoom-in for details.

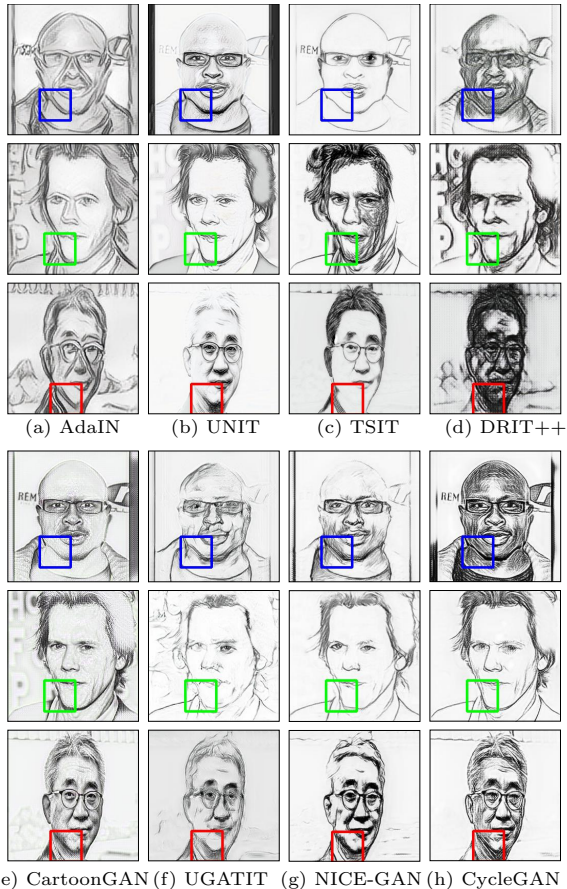


Fig. 9 Comparison of AdaIN [123], UNIT [22], TSIT [80], DRIT++ [27], CartoonGAN [85], UGATIT [30], NICE-GAN [26], and CycleGAN [21]. Their inputs and references are shown in Fig. 8.

CartoonGAN [85], UGATIT [30], NICE-GAN [26], and CycleGAN [21], whose SCOOT scores range from 0.3 to 0.35. As shown in Fig. 9, the synthesized sketch images are better in terms of structure-preservation compared to the first group. However, except for AdaIN, all models are thrown off by the complex backgrounds (see the hair region in the second row). Besides, the results of CartoonGAN seem to alter the color of the input images, leading to lower SSIM scores.

MDAL [11], UPDG [9], Pix2pixHD [23], APDrawing [2], DSMAP [25], and our FSGAN are categorized into the third group, which can generate sketches without distortion or losing too much of the global details. However, UPDG and APDrawing miss some details in the hair region, leading to poor visual effects. APDrawing introduces many extra strokes, especially for the first sketch style. Besides, APDrawing usually results in a lack and distortion of the local structure, as seen in the hair region. Meanwhile, the sketches generated by UPDG have better style elements, but the model cannot handle complex backgrounds. Pix2pixHD generates relatively good sketches with global structure and clean background, but it does not generate the best facial components. For example, in Fig. 10-e, the region around the eyes is unclear, and many details are lost. Take the third row, for instance; the eyeglasses are partially lost, while the eyeball is entirely black. We further observe that DSMAP and MDAL tend to achieve better sketch images but with distortions in local facial information.

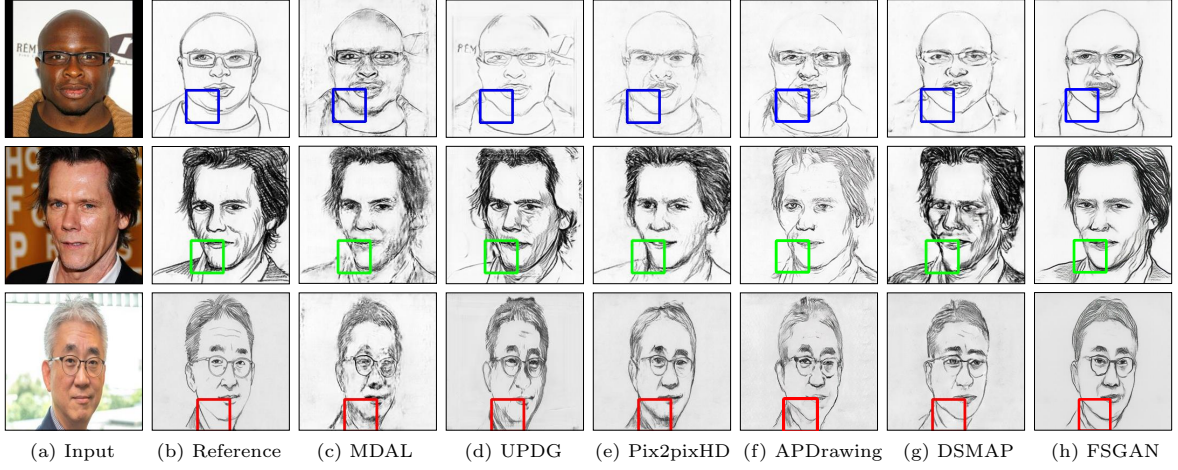


Fig. 10 Comparison results with MDAL [11], UPDG [9], Pix2pixHD [23], APDrawing [2], and DSMAP [25].

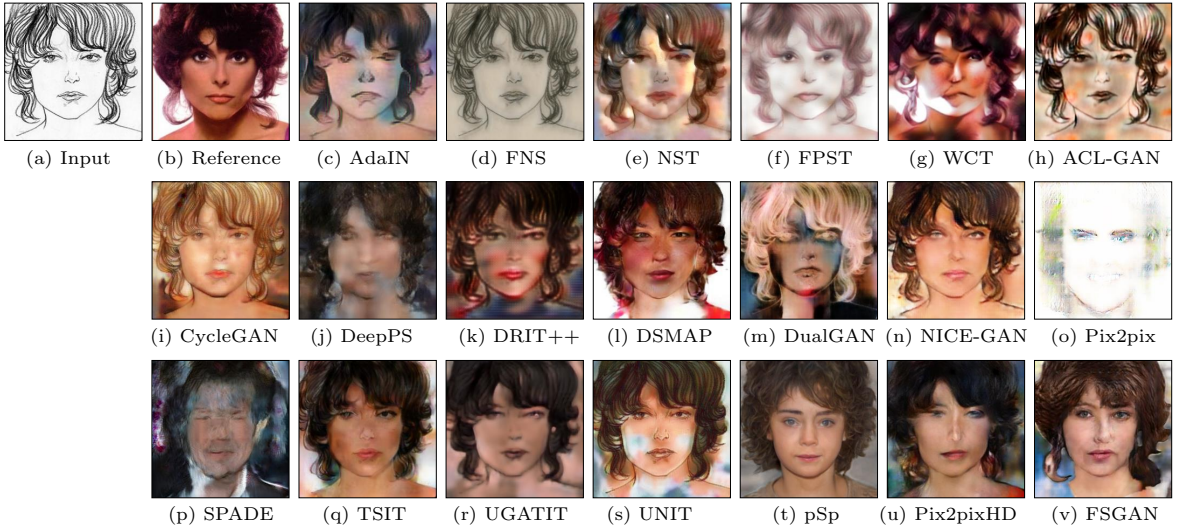


Fig. 11 We select 19 classical models, including AdaIN [123], FNS [93], FPST [95], WCT [124], ACL-GAN [79], CycleGAN [21], DeepPS [148], DRIT++ [27], DSMAP [25], DualGAN [78], NICE-GAN [26], Pix2pix [31], SPADE [24], TSIT [80], UGATIT [30], UNIT [22], pSp [86], and Pix2pixHD [23], for qualitative comparison.

Finally, the baseline can synthesize high-quality sketches that focus on the global structure and local details while considering diverse styles. Moreover, as shown in the highlighted boxes (with green, blue and red), we find that the outputs of the FSGAN are more similar to the reference compared to other state-of-the-arts methods.

5.2.2 S2I Task

We report our experimental results in Table 6 and Fig. 11. We find that FSGAN achieves the best results on our challenging FS2K compared to the existing state-of-the-art models.

Analysis. As seen in Fig. 11, we observe that most compared methods are unable to successfully recover accurate images, revealing that the S2I task is more complicated than I2S. We argue that this is because the sketches are highly abstract, and the loss of valuable information makes it difficult for neural networks to restore the original image. We also observe that the high-resolution models, such as Pix2pixHD and FSGAN, tend to output more visually appealing results.

The results presented in Fig. 11 show that FNS and FPST fail to transfer the sketches into colored images. SPADE and Pix2pix generate poor results with facial outlines (*e.g.*, Pix2pix)

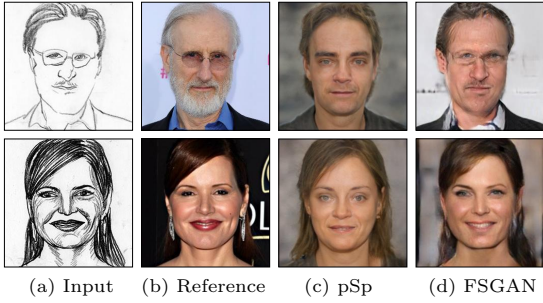


Fig. 12 Visual diversity of the data generated for S2I task.

or black background (*e.g.*, SPADE). Five models (*i.e.*, NST, WCT, DeepPS, DSMAP, and UNIT) produce noise patches in salient regions, which corrupt the global facial structure. Meanwhile, AdaIN, ACL-GAN, DualGAN, and UGATIT perform better than the models mentioned above, resulting in unrealistic cartoon-style images. Only CycleGAN, NICE-GAN, TSIT, pSp, and Pix2pixHD overcome various challenges and achieve good results in terms of facial completeness. In particular, the eye regions from Pix2pixHD [23] and pSp [86] are better than those from the other models. However, compared with the results of the FSGAN, the facial features of Pix2pixHD are relatively inferior because a pixel-wise rather than block-wise strategy learns. Although pSp [86] can generate high-quality results, its results lack diversity compared with the FSGAN baseline. For example, pSp generates similar facial expressions under two different sketch styles, while the baseline can synthesize diverse contents, as shown in Fig. 12.

5.3 Attribute-Based Analysis

5.3.1 SCOOT Metric Results

To provide a deeper understanding of the models, we present an attribute-based performance evaluation in Table 7.

Analysis. Hair is one of the dominant features of the head. In Table 7, we find that most models achieve slightly better or comparable performance on images without hair than with, except for three models, such as AdaIN, CartoonGAN, and CycleGAN. Meanwhile, we find that red and black hair are the most challenging and easiest to detect/reconstruct, respectively. We argue that this is because images with red and black hair make up the lowest and largest ($>40\%$) proportion

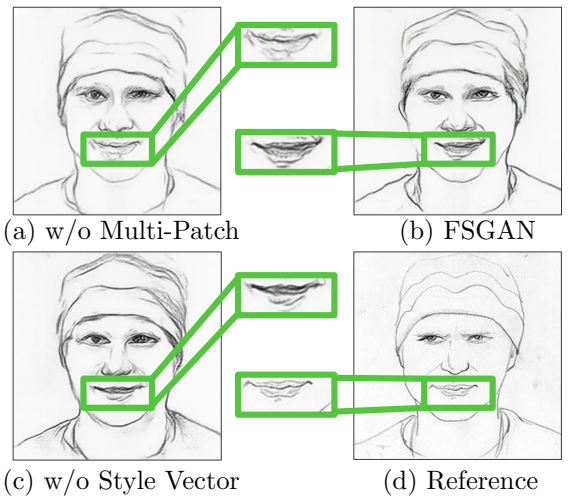


Fig. 13 Ablation study for the I2S task.

of all data, respectively. Thus, the models are unfamiliar/familiar with these attributes.

In addition, we also notice that females (F) are more challenging than males (M) for almost all models since women usually have various accessories and hairstyles. For example, the models perform worse on images with earrings (w/ E) than those without earrings. Additionally, facial images with smiles are more challenging than those without smiles. Interestingly, existing models achieve diverse performance irrespective of the color of hair (*e.g.*, H(b), H(bl), H(r), and H(g)). Finally, compared to style 1 (simple lines) and style 3 (*i.e.*, repeated wispy details), we see that style 2 (long strokes) is the most challenging for all models.

5.3.2 SSIM Metric Results

In addition to the SCOOT metric, we also provide the SSIM metric for the I2S task in Table 8.

Analysis. We find that the overall performance tends to be similar to the SCOOT metric results in several key attributes, such as hair, gender, accessories, and style. We note that the performance on “w/ F” is lower than on “w/o F”, as shown in Table 8. One possible reason is that frontal faces preserve more structural features than non-frontal faces. Therefore, in the I2S task, images with attributes such as “w/ F” are more challenging than “w/o F”.

Table 7 Comparison of 19 state-of-the-art models in terms of attribute-based performance on the I2S task. Here, w/ H = hair visible, w/o H = hair invisible, H(b) = brown hair, H(bl) = black hair, H(r) = red hair, H(g) = golden hair, M = male, F = female, w/ E = with earring, w/o E = without earring, w/ S = with smile, w/o S = without smile, w/ F = frontal face, w/o F = non-frontal face, S1 = style1, S2 = style2, and S3 = style3.

Model	SCOOT↑																
	w/ H	w/o H	H(b)	H(bl)	H(r)	H(g)	M	F	w/ E	w/o E	w/ S	w/o S	w/ F	w/o F	S1	S2	S3
DualGAN [78]	0.260	0.279	0.250	0.267	0.216	0.279	0.275	0.240	0.239	0.266	0.255	0.271	0.261	0.262	0.298	0.194	0.319
FPST [95]	0.269	0.304	0.254	0.294	0.214	0.304	0.288	0.245	0.246	0.276	0.262	0.286	0.269	0.278	0.329	0.168	0.332
NST [87, 88]	0.272	0.283	0.268	0.287	0.236	0.283	0.280	0.262	0.258	0.276	0.268	0.282	0.272	0.276	0.310	0.205	0.332
Pix2pix [31]	0.272	0.335	0.255	0.300	0.217	0.335	0.298	0.240	0.250	0.281	0.267	0.290	0.276	0.272	0.333	0.178	0.302
ACL-GAN [79]	0.276	0.309	0.265	0.298	0.226	0.309	0.292	0.256	0.254	0.283	0.270	0.291	0.276	0.284	0.330	0.183	0.355
WCT [124]	0.281	0.315	0.271	0.302	0.229	0.315	0.296	0.261	0.262	0.287	0.277	0.292	0.281	0.290	0.332	0.195	0.346
AdaIN [123]	0.303	0.295	0.307	0.317	0.258	0.295	0.306	0.298	0.283	0.307	0.298	0.310	0.300	0.314	0.348	0.215	0.419
UNIT [22]	0.301	0.364	0.292	0.328	0.225	0.364	0.330	0.265	0.261	0.313	0.293	0.324	0.301	0.319	0.376	0.175	0.411
TSIT [80]	0.307	0.307	0.308	0.320	0.259	0.307	0.320	0.288	0.283	0.313	0.300	0.320	0.306	0.316	0.359	0.208	0.432
DRIT++ [27]	0.305	0.348	0.291	0.336	0.248	0.348	0.329	0.276	0.279	0.314	0.299	0.323	0.305	0.323	0.380	0.181	0.378
CartoonGAN [85]	0.319	0.318	0.320	0.337	0.262	0.318	0.329	0.304	0.291	0.325	0.314	0.329	0.317	0.332	0.382	0.204	0.428
UGATIT [30]	0.321	0.365	0.315	0.347	0.265	0.365	0.339	0.298	0.298	0.328	0.314	0.338	0.322	0.325	0.391	0.204	0.400
NICE-GAN [26]	0.325	0.355	0.320	0.357	0.262	0.355	0.342	0.303	0.302	0.332	0.317	0.343	0.325	0.333	0.398	0.201	0.401
CycleGAN [21]	0.348	0.343	0.358	0.362	0.287	0.343	0.351	0.343	0.326	0.353	0.341	0.360	0.346	0.357	0.397	0.252	0.483
MDAL [11]	0.354	0.363	0.348	0.380	0.292	0.363	0.369	0.333	0.329	0.360	0.345	0.372	0.352	0.365	0.436	0.211	0.446
UPDG [9]	0.362	0.411	0.349	0.390	0.290	0.411	0.390	0.325	0.336	0.371	0.356	0.379	0.363	0.370	0.423	0.259	0.448
APDrawing [2]	0.374	0.395	0.372	0.399	0.322	0.395	0.380	0.369	0.356	0.380	0.370	0.385	0.373	0.390	0.456	0.227	0.524
Pix2pixHD [23]	0.374	0.392	0.365	0.403	0.307	0.385	0.392	0.351	0.343	0.378	0.371	0.392	0.371	0.381	0.462	0.212	0.508
DSMAP [25]	0.375	0.431	0.357	0.405	0.322	0.431	0.400	0.343	0.354	0.383	0.369	0.393	0.377	0.381	0.437	0.276	0.423
FSGAN	0.403	0.435	0.389	0.435	0.335	0.435	0.423	0.377	0.381	0.410	0.395	0.422	0.403	0.414	0.481	0.268	0.509

Table 8 Comparison of 19 top models in terms of attribute-based performance on the I2S task.

Model	SSIM↑																
	w/ H	w/o H	H(b)	H(bl)	H(r)	H(g)	M	F	w/ E	w/o E	w/ S	w/o S	w/ F	w/o F	S1	S2	S3
DualGAN [78]	0.320	0.393	0.310	0.342	0.276	0.393	0.352	0.282	0.292	0.331	0.313	0.343	0.318	0.354	0.364	0.247	0.424
FPST [95]	0.459	0.481	0.442	0.492	0.383	0.481	0.492	0.411	0.416	0.469	0.448	0.481	0.455	0.486	0.517	0.351	0.597
NST [87, 88]	0.325	0.347	0.317	0.349	0.256	0.347	0.339	0.306	0.305	0.330	0.316	0.344	0.324	0.338	0.372	0.241	0.417
Pix2pix [31]	0.434	0.526	0.410	0.470	0.332	0.526	0.478	0.377	0.391	0.449	0.425	0.461	0.438	0.439	0.503	0.319	0.558
ACL-GAN [79]	0.402	0.432	0.392	0.430	0.334	0.432	0.427	0.369	0.363	0.413	0.393	0.423	0.398	0.434	0.445	0.316	0.583
WCT [124]	0.368	0.389	0.368	0.387	0.316	0.389	0.389	0.339	0.334	0.377	0.362	0.381	0.367	0.380	0.407	0.297	0.461
AdaIN [123]	0.364	0.367	0.364	0.382	0.319	0.367	0.378	0.343	0.340	0.370	0.359	0.375	0.362	0.379	0.399	0.297	0.460
UNIT [22]	0.501	0.556	0.488	0.528	0.421	0.556	0.539	0.450	0.460	0.514	0.492	0.526	0.498	0.532	0.563	0.395	0.616
TSIT [80]	0.439	0.465	0.430	0.461	0.371	0.465	0.465	0.404	0.408	0.448	0.431	0.458	0.435	0.468	0.485	0.351	0.587
DRIT++ [27]	0.490	0.534	0.479	0.519	0.411	0.534	0.524	0.444	0.451	0.501	0.480	0.512	0.487	0.515	0.547	0.387	0.617
CartoonGAN [85]	0.399	0.420	0.397	0.421	0.345	0.420	0.419	0.372	0.368	0.407	0.392	0.416	0.395	0.425	0.438	0.321	0.552
UGATIT [30]	0.455	0.497	0.445	0.476	0.386	0.497	0.489	0.409	0.416	0.466	0.447	0.476	0.451	0.491	0.499	0.373	0.593
NICE-GAN [26]	0.472	0.497	0.463	0.492	0.398	0.497	0.505	0.424	0.429	0.483	0.464	0.490	0.468	0.498	0.518	0.384	0.603
CycleGAN [21]	0.433	0.461	0.429	0.455	0.374	0.461	0.460	0.395	0.401	0.442	0.425	0.452	0.429	0.463	0.471	0.358	0.580
MDAL [11]	0.465	0.487	0.457	0.491	0.399	0.487	0.496	0.420	0.426	0.475	0.458	0.481	0.462	0.488	0.506	0.386	0.593
UPDG [9]	0.468	0.507	0.456	0.500	0.391	0.507	0.501	0.424	0.431	0.479	0.459	0.493	0.465	0.501	0.534	0.355	0.584
APDrawing [2]	0.461	0.522	0.441	0.497	0.373	0.522	0.504	0.402	0.419	0.473	0.452	0.484	0.458	0.492	0.512	0.371	0.582
Pix2pixHD [23]	0.492	0.552	0.473	0.523	0.419	0.546	0.531	0.431	0.457	0.505	0.481	0.513	0.488	0.524	0.537	0.402	0.618
DSMAP [25]	0.490	0.551	0.472	0.527	0.405	0.551	0.532	0.433	0.447	0.503	0.481	0.515	0.488	0.518	0.557	0.373	0.622
FSGAN	0.507	0.565	0.491	0.539	0.424	0.565	0.549	0.451	0.466	0.520	0.498	0.531	0.505	0.534	0.568	0.403	0.629

5.4 Ablation Study

This section provides a detailed analysis of FSGAN on the proposed FS2K dataset. Unlike most existing facial synthesis models [23], our model has a two-stage GAN architecture for both I2S and S2I tasks. Besides, a sketch style vector is introduced to enable diversified style synthesis in the second stage of the I2S task. Therefore, the ablation studies on the I2S task are conducted on the following two key components: (1) the facial components synthesis stage and (2) the style

vector assisted generation. Note that we adopt the same hyperparameters described in Sec. 4.5 during our ablation experiments.

Table 9 shows the ablation results for the I2S task. We find that the facial components synthesis stage increases the SCOOT and SSIM scores by 1.31% (relative) and 2.67%, respectively, while the style vector increases them by 6.30% and 4.72%. As illustrated in Fig. 13, without the multi-patch strategy, the lines in the synthesized lips are often missing structural details. Meanwhile, with the multi-patch stage, the lines become smoother.



(a) Input (b) w/o multi-patch (c) FSGAN

Fig. 14 Ablation study for the S2I task.

Table 9 Ablation study of FSGAN on the I2S task.

Setting	multi-patch	style vec.	SCOOT↑	SSIM↑
Baseline			0.381	0.487
FSGAN	✓	✓	0.386 (+1.31%)	0.500 (+2.67%)
			0.405 (+6.30%)	0.510 (+4.72%)

Moreover, the synthesized drawings are messier without the style vector component and may introduce shadows in the lip regions.

For the S2I task, an ablation study is conducted to validate the effectiveness of the facial component synthesis stage, as shown in Table 10. Similar to the I2S task, the multi-patch component achieves a significant performance gain (*i.e.*, 3.3%) over the baseline model. Fig. 14 provides examples of the results produced by our model and the model without the facial components synthesis stage. Our model with facial component synthesis captures more details and ensures a more realistic overall appearance (see Fig. 14-c).

6 Discussion

Although FSS has achieved significant progress, there is still a large room for improvement. This section summarizes the possible future research directions related to FSS.

(1) Datasets. Due to the relative shortage of professional sketch artists, achieving large numbers of images remains an open problem, impeding the development of FSS. Furthermore, more diversified sketch (or drawing) styles are needed to build more attractive models and achieve better synthesis results. To address these issues, we believe novel data augmentation techniques [111, 184, 185] and transfer learning strategies [186–188] designed for FSS are promising directions of study.

(2) Models. Currently, most state-of-the-art models are trained with a large number of paired images, and sketches [9, 23] to

Table 10 Ablation study of our model on the S2I task.

Setting	multi-patch	SSIM↑
Baseline		0.487
FSGAN	✓	0.503 (+3.3%)

overcome data shortages. However, more attention could be paid to techniques such as few-shot [189], semi-supervised [190], weakly-supervised [191], self-supervised [192], and non-pairwise unsupervised [83] learning to achieve style transfer with limited datasets. Besides, developing novel, human-in-the-loop [193] models is another promising direction, that would provide more interactive options to users for generating and editing personalized styles. Interactive models that utilize the attributes in our FS2K could also serve as drawing tools provided to professional artists for facilitating the creation of sketches and other styles of drawing. Furthermore, FSS in the wild is still challenging because the image quality, including resolution, noise, and background, varies drastically. In addition to the techniques mentioned above, basic model units could also be focused on to develop new strategies. For example, most current models are built upon CNN [194] units. Therefore, more exploration of other frameworks, such as MLPs [195] and Transformers [196, 197], could also be conducted.

(3) Evaluation. Evaluation metrics are essential for the development of new models and the benchmarking of existing models. Currently, several quantitative evaluation metrics [20, 198] and human visual ranking methods [66] are used. However, as these aim to provide relatively objective and fair comparisons between all models, the different applications of FSS are not considered. This may lead to biased or unreliable evaluation of specific tasks. Therefore, more task-specific evaluation metrics and methods could be another important direction for future research.

(4) Applications. Currently, the only direct applications of FSS (I2S and S2I) are entertainment, and law enforcement [1, 44]. With the development of FSS techniques, many other promising applications could also be implicitly or explicitly facilitated by FSS research, such as art design and animation production. In addition to these industrial applications, we believe that FSS methods and ideas could also benefit other research fields. For example, sketches

could be used to assist image resizing [199], super-resolution [200], *etc.* Further, the sketches usually contain the most conspicuous information of an image and can therefore be considered compressed versions of RGB images [201]. This characteristic makes sketches useful for the image compression task. Besides, the S2I task can be considered a specific case of image super-resolution in a broad sense because both tasks aim to reconstruct detailed RGB images from the given inputs. The difference is that the input of S2I is high-frequency information, while that of the standard super-resolution task is the low-frequency information of the original image.

7 Conclusion

We have presented a complete review of the facial-sketch synthesis problem. To the best of our knowledge, this is the first systematic study on deep FSS in sketch-to-image and image-to-sketch tasks. To achieve this, we established a new challenging dataset, named FS2K. We also introduced a copy table for the proposed FS2K to address the alignment issue between the sketches drawn by artists and the original images. The proposed simple baseline, FSGAN, achieves the new state-of-the-art performance with a two-stage architecture. Finally, as the most extensive survey (*i.e.*, 89 literature methods) and benchmark (*i.e.*, 19 cutting-edge models), we have revealed that the development of this field is still in its infancy. Therefore, the main goal of this paper is to spark novel ideas rather than rank all existing models. It is not easy to benchmark all of the existing models due to the prosperity of the field. We hope this investigation will attract the community's attention and yield exciting follow-up directions, such as generating vivid sketches with music, developing cartoons from sketches, synthesizing sketch videos, and fake faces [202].

Conflicts of Interests

The authors declare that they have no conflicts of interest to this work. We declare that we do not have any commercial or associative interest that represents a conflict of interest in connection with the work submitted.

References

- [1] X. Wang and X. Tang, “Face photo-sketch synthesis and recognition,” *IEEE Transactions on pattern analysis and machine intelligence*, vol. 31, no. 11, pp. 1955–1967, 2008.
- [2] R. Yi, Y.-J. Liu, Y.-K. Lai, and P. L. Rosin, “APDrawingGAN: Generating artistic portrait drawings from face photos with hierarchical GANs,” in *Conference on computer vision and pattern recognition*. IEEE, 2019, pp. 10743–10752.
- [3] H. Koshimizu, M. Tominaga, T. Fujiwara, and K. Murakami, “On kansei facial image processing for computerized facial caricaturing system picasso,” in *International Conference on Systems, Man, and Cybernetics*. IEEE, 1999, pp. 294–299.
- [4] H. S. Bhatt, S. Bharadwaj, R. Singh, and M. Vatsa, “On matching sketches with digital face images,” in *International Conference on Biometrics: Theory, Applications and Systems*. IEEE, 2010, pp. 1–7.
- [5] W. Zhang, X. Wang, and X. Tang, “Coupled information-theoretic encoding for face photo-sketch recognition,” in *Conference on computer vision and pattern recognition*. IEEE, 2011, pp. 513–520.
- [6] N. Wang, X. Gao, D. Tao, and X. Li, “Face sketch-photo synthesis under multi-dictionary sparse representation framework,” in *International Conference on Image and Graphics*. IEEE, 2011, pp. 82–87.
- [7] X. Gao, N. Wang, D. Tao, and X. Li, “Face sketch-photo synthesis and retrieval using sparse representation,” *IEEE Transactions on circuits and systems for video technology*, vol. 22, no. 8, pp. 1213–1226, 2012.
- [8] I. Berger, A. Shamir, M. Mahler, E. Carter, and J. Hodgins, “Style and abstraction in portrait sketching,” *ACM Transactions on graphics*, vol. 32, no. 4, pp. 1–12, 2013.

[9] R. Yi, Y.-J. Liu, Y.-K. Lai, and P. L. Rosin, “Unpaired portrait drawing generation via asymmetric cycle mapping,” in *Conference on computer vision and pattern recognition*. IEEE, 2020, pp. 8217–8225.

[10] R. Yi, M. Xia, Y.-J. Liu, Y.-K. Lai, and P. L. Rosin, “Line drawings for face portraits from photos using global and local structure based GANs,” *IEEE Transactions on pattern analysis and machine intelligence*, vol. 43, no. 10, pp. 3462–3475, 2020.

[11] S. Zhang, R. Ji, J. Hu, X. Lu, and X. Li, “Face sketch synthesis by multidomain adversarial learning,” *IEEE Transactions on Neural Networks and Learning Systems*, vol. 30, no. 5, pp. 1419–1428, 2018.

[12] M. Zhu, J. Li, N. Wang, and X. Gao, “Knowledge distillation for face photo-sketch synthesis,” *IEEE Transactions on Neural Networks and Learning Systems*, vol. 33, no. 2, pp. 893–906, 2022.

[13] N. Kumar, A. C. Berg, P. N. Belhumeur, and S. K. Nayar, “Attribute and simile classifiers for face verification,” in *International conference on computer vision*. IEEE, 2009, pp. 365–372.

[14] H.-S. Du, Q.-P. Hu, D.-F. Qiao, and I. Pitas, “Robust face recognition via low-rank sparse representation-based classification,” *International Journal of Automation and Computing*, vol. 12, no. 6, pp. 579–587, 2015.

[15] Y.-Z. Lu, “A novel face recognition algorithm for distinguishing faces with various angles,” *International Journal of Automation and Computing*, vol. 5, no. 2, pp. 193–197, 2008.

[16] V. Jain and E. Learned-Miller, “Fddb: A benchmark for face detection in unconstrained settings,” UMass Amherst technical report, Tech. Rep., 2010.

[17] Z. Zhang, P. Luo, C. C. Loy, and X. Tang, “Facial landmark detection by deep multi-task learning,” in *European conference on computer vision*. Springer, 2014, pp. 94–108.

[18] A. Bulat and G. Tzimiropoulos, “How far are we from solving the 2d & 3d face alignment problem?(and a dataset of 230,000 3d facial landmarks),” in *International conference on computer vision*. IEEE, 2017, pp. 1021–1030.

[19] J. Sun, Q. Li, W. Wang, J. Zhao, and Z. Sun, “Multi-caption text-to-face synthesis: Dataset and algorithm,” in *International conference on Multimedia*. ACM, 2021, pp. 2290–2298.

[20] Z. Wang, A. C. Bovik, H. R. Sheikh, and E. P. Simoncelli, “Image quality assessment: from error visibility to structural similarity,” *IEEE Transactions on image processing*, vol. 13, no. 4, pp. 600–612, 2004.

[21] J.-Y. Zhu, T. Park, P. Isola, and A. A. Efros, “Unpaired image-to-image translation using cycle-consistent adversarial networks,” in *International conference on computer vision*. IEEE, 2017, pp. 2223–2232.

[22] M.-Y. Liu, T. Breuel, and J. Kautz, “Unsupervised image-to-image translation networks,” in *Advances in neural information processing systems*. Curran Associates, Inc., 2017.

[23] T.-C. Wang, M.-Y. Liu, J.-Y. Zhu, A. Tao, J. Kautz, and B. Catanzaro, “High-resolution image synthesis and semantic manipulation with conditional GANs,” in *Conference on computer vision and pattern recognition*. IEEE, 2018, pp. 8798–8807.

[24] T. Park, M.-Y. Liu, T.-C. Wang, and J.-Y. Zhu, “Semantic image synthesis with spatially-adaptive normalization,” in *Conference on computer vision and pattern recognition*. IEEE, 2019, pp. 2337–2346.

[25] H.-Y. Chang, Z. Wang, and Y.-Y. Chuang, “Domain-specific mappings for generative adversarial style transfer,” in *European conference on computer vision*. Springer, 2020, pp. 573–589.

[26] R. Chen, W. Huang, B. Huang, F. Sun, and B. Fang, “Reusing discriminators for encoding: Towards unsupervised image-to-image translation,” in *Conference on computer vision and pattern recognition*. IEEE, 2020, pp. 8168–8177.

[27] H.-Y. Lee, H.-Y. Tseng, Q. Mao, J.-B. Huang, Y.-D. Lu, M. Singh, and M.-H. Yang, “Drit++: Diverse image-to-image translation via disentangled representations,” *International journal of computer vision*, vol. 128, no. 10, pp. 2402–2417, 2020.

[28] Z. Liu, P. Luo, X. Wang, and X. Tang, “Deep learning face attributes in the wild,” in *International conference on computer vision*. IEEE, 2015, pp. 3730–3738.

[29] D.-P. Fan, S. Zhang, Y.-H. Wu, Y. Liu, M.-M. Cheng, B. Ren, P. L. Rosin, and R. Ji, “Scoot: A perceptual metric for facial sketches,” in *International conference on computer vision*. IEEE, 2019, pp. 5612–5622.

[30] J. Kim, M. Kim, H. Kang, and K. Lee, “U-gat-it: unsupervised generative attentional networks with adaptive layer-instance normalization for image-to-image translation,” in *International Conference on Learning Representations*. OpenReview.net, 2020.

[31] P. Isola, J.-Y. Zhu, T. Zhou, and A. A. Efros, “Image-to-image translation with conditional adversarial networks,” in *Conference on computer vision and pattern recognition*. IEEE, 2017, pp. 1125–1134.

[32] C. Peng, X. Gao, N. Wang, and J. Li, “Face recognition from multiple stylistic sketches: Scenarios, datasets, and evaluation,” *Pattern Recognition*, vol. 84, pp. 262–272, 2018.

[33] A. M. Martinez, “The ar face database,” *CVC Technical Report24*, 1998.

[34] K. Messer, J. Matas, J. Kittler, J. Luettin, G. Maitre *et al.*, “XM2VTSDB: The extended m2vts database,” in *International conference on audio and video-based biometric person authentication*, vol. 964. Springer, 1999, pp. 965–966.

[35] P. J. Phillips, H. Moon, S. A. Rizvi, and P. J. Rauss, “The FERET evaluation methodology for face-recognition algorithms,” *IEEE Transactions on pattern analysis and machine intelligence*, vol. 22, no. 10, pp. 1090–1104, 2000.

[36] Á. Serrano, I. M. de Diego, C. Conde, E. Cabello, L. Shen, and L. Bai, “Influence of wavelet frequency and orientation in an SVM-based parallel gabor PCA face verification system,” in *International Conference on Intelligent Data Engineering and Automated Learning*. Springer, 2007, pp. 219–228.

[37] H. S. Bhatt, S. Bharadwaj, R. Singh, and M. Vatsa, “Memetically optimized MCWLD for matching sketches with digital face images,” *Transactions on Information Forensics and Security*, vol. 7, no. 5, pp. 1522–1535, 2012.

[38] M. Minear and D. C. Park, “A lifespan database of adult facial stimuli,” *Behavior research methods, instruments, & computers*, vol. 36, no. 4, pp. 630–633, 2004.

[39] J. Nishino, T. Kamyama, H. Shira, T. Odaka, and H. Ogura, “Linguistic knowledge acquisition system on facial caricature drawing system,” in *International Fuzzy Systems*. IEEE, 1999, pp. 1591–1596.

[40] S. Iwashita, Y. Takeda, and T. Onisawa, “Expressive facial caricature drawing,” in *International Fuzzy Systems*. IEEE, 1999, pp. 1597–1602.

[41] Y. Li and H. Kobatake, “Extraction of facial sketch image based on morphological processing,” in *International Conference on Image Processing*. IEEE, 1997, pp. 316–319.

[42] M. Tominaga, S. Fukuoka, K. Murakami, and H. Koshimizu, “Facial caricaturing with

motion caricaturing in PICASSO system," in *International Conference on Advanced Intelligent Mechatronics*. IEEE, 1997, p. 30.

[43] S. E. Brennan, "Caricature generator," Ph.D. dissertation, Massachusetts Institute of Technology, 1982.

[44] N. Wang, D. Tao, X. Gao, X. Li, and J. Li, "A comprehensive survey to face hallucination," *International journal of computer vision*, vol. 106, no. 1, pp. 9–30, 2014.

[45] H. Chen, Y.-Q. Xu, H.-Y. Shum, S.-C. Zhu, and N.-N. Zheng, "Example-based facial sketch generation with non-parametric sampling," in *International conference on computer vision*. IEEE, 2001, pp. 433–438.

[46] A. V. Nefian and M. H. Hayes III, "Face recognition using an embedded hmm," in *Conference on Audio and Video-based Biometric Person Authentication*. IEEE, 1999.

[47] X. Gao, J. Zhong, J. Li, and C. Tian, "Face sketch synthesis algorithm based on e-hmm and selective ensemble," *IEEE Transactions on circuits and systems for video technology*, vol. 18, no. 4, pp. 487–496, 2008.

[48] Z. Xu, H. Chen, S.-C. Zhu, and J. Luo, "A hierarchical compositional model for face representation and sketching," *IEEE Transactions on pattern analysis and machine intelligence*, vol. 30, no. 6, pp. 955–969, 2008.

[49] W. Zhang, X. Wang, and X. Tang, "Lighting and pose robust face sketch synthesis," in *European conference on computer vision*. Springer, 2010, pp. 420–433.

[50] H. Zhou, Z. Kuang, and K.-Y. K. Wong, "Markov weight fields for face sketch synthesis," in *Conference on computer vision and pattern recognition*. IEEE, 2012, pp. 1091–1097.

[51] T. Wang, J. P. Collomosse, A. Hunter, and D. Greig, "Learnable stroke models for example-based portrait painting," in *British Machine Vision Conference*. BMVA Press, 2013.

[52] N. Wang, D. Tao, X. Gao, X. Li, and J. Li, "Transductive face sketch-photo synthesis," *IEEE Transactions on Neural Networks and Learning Systems*, vol. 24, no. 9, pp. 1364–1376, 2013.

[53] C. Peng, X. Gao, N. Wang, and J. Li, "Superpixel-based face sketch-photo synthesis," *IEEE Transactions on circuits and systems for video technology*, vol. 27, no. 2, pp. 288–299, 2015.

[54] C. Peng, X. Gao, N. Wang, D. Tao, X. Li, and J. Li, "Multiple representations-based face sketch-photo synthesis," *IEEE Transactions on Neural Networks and Learning Systems*, vol. 27, no. 11, pp. 2201–2215, 2015.

[55] H. Abdi and L. J. Williams, "Principal component analysis," *Wiley interdisciplinary reviews: computational statistics*, vol. 2, no. 4, pp. 433–459, 2010.

[56] X. Tang and X. Wang, "Face photo recognition using sketch," in *International Conference on Image Processing*. IEEE, 2002, pp. I–I.

[57] X. Tang and X. Wang, "Face sketch synthesis and recognition," in *International conference on computer vision*. IEEE, 2003, pp. 687–694.

[58] X. Tang and X. Wang, "Face sketch recognition," *IEEE Transactions on circuits and systems for video technology*, vol. 14, no. 1, pp. 50–57, 2004.

[59] Q. Liu, X. Tang, H. Jin, H. Lu, and S. Ma, "A nonlinear approach for face sketch synthesis and recognition," in *Conference on computer vision and pattern recognition*. IEEE, 2005, pp. 1005–1010.

[60] D.-A. Huang and Y.-C. F. Wang, "Coupled dictionary and feature space learning with applications to cross-domain image

synthesis and recognition,” in *International conference on computer vision*. IEEE, 2013, pp. 2496–2503.

[61] N. Ji, X. Chai, S. Shan, and X. Chen, “Local regression model for automatic face sketch generation,” in *International Conference on Image and Graphics*. IEEE, 2011, pp. 412–417.

[62] L. Chang, M. Zhou, X. Deng, Z. Wu, and Y. Han, “Face sketch synthesis via multivariate output regression,” in *International conference on human-computer interaction*. Springer, 2011, pp. 555–561.

[63] J. Zhang, N. Wang, X. Gao, D. Tao, and X. Li, “Face sketch-photo synthesis based on support vector regression,” in *International Conference on Image Processing*. IEEE, 2011, pp. 1125–1128.

[64] S. T. Roweis and L. K. Saul, “Nonlinear dimensionality reduction by locally linear embedding,” *Science*, vol. 290, no. 5500, pp. 2323–2326, 2000.

[65] S. Wang, L. Zhang, Y. Liang, and Q. Pan, “Semi-coupled dictionary learning with applications to image super-resolution and photo-sketch synthesis,” in *Conference on computer vision and pattern recognition*. IEEE, 2012, pp. 2216–2223.

[66] Y. Song, L. Bao, Q. Yang, and M.-H. Yang, “Real-time exemplar-based face sketch synthesis,” in *European conference on computer vision*. Springer, 2014, pp. 800–813.

[67] N. Wang, X. Gao, and J. Li, “Random sampling for fast face sketch synthesis,” *Pattern Recognition*, vol. 76, pp. 215–227, 2018.

[68] S. Zhang, X. Gao, N. Wang, and J. Li, “Robust face sketch style synthesis,” *IEEE Transactions on image processing*, vol. 25, no. 1, pp. 220–232, 2015.

[69] Y. Li, Y.-Z. Song, T. M. Hospedales, and S. Gong, “Free-hand sketch synthesis with deformable stroke models,” *International journal of computer vision*, vol. 122, no. 1, pp. 169–190, 2017.

[70] J. Li, X. Yu, C. Peng, and N. Wang, “Adaptive representation-based face sketch-photo synthesis,” *Neurocomputing*, vol. 269, pp. 152–159, 2017.

[71] Y. Men, Z. Lian, Y. Tang, and J. Xiao, “A common framework for interactive texture transfer,” in *Conference on computer vision and pattern recognition*. IEEE, 2018, pp. 6353–6362.

[72] S. Saxena and M. N. Teli, “Comparison and analysis of image-to-image generative adversarial networks: A survey,” *arXiv preprint arXiv:2112.12625*, 2021.

[73] I. J. Goodfellow, J. Pouget-Abadie, M. Mirza, B. Xu, D. Warde-Farley, S. Ozair, A. Courville, and Y. Bengio, “Generative adversarial networks,” in *Advances in neural information processing systems*. Curran Associates, Inc., 2014.

[74] M. Mirza and S. Osindero, “Conditional generative adversarial nets,” in *Advances in neural information processing systems workshops*. Curran Associates, Inc., 2014.

[75] O. Ronneberger, P. Fischer, and T. Brox, “U-net: Convolutional networks for biomedical image segmentation,” in *Medical Image Computing and Computer Assisted Intervention*. Springer, 2015, pp. 234–241.

[76] J.-Y. Zhu, R. Zhang, D. Pathak, T. Darrell, A. A. Efros, O. Wang, and E. Shechtman, “Toward multimodal image-to-image translation,” in *Advances in neural information processing systems*. Curran Associates, Inc., 2017.

[77] T. Kim, M. Cha, H. Kim, J. K. Lee, and J. Kim, “Learning to discover cross-domain relations with generative adversarial networks,” in *International conference on machine learning*. PMLR, 2017, pp.

1857–1865.

[78] Z. Yi, H. Zhang, P. Tan, and M. Gong, “DualGAN: Unsupervised dual learning for image-to-image translation,” in *International conference on computer vision*. IEEE, 2017, pp. 2849–2857.

[79] Y. Zhao, R. Wu, and H. Dong, “Unpaired image-to-image translation using adversarial consistency loss,” in *European conference on computer vision*. Springer, 2020, pp. 800–815.

[80] L. Jiang, C. Zhang, M. Huang, C. Liu, J. Shi, and C. C. Loy, “TSIT: A simple and versatile framework for image-to-image translation,” in *European conference on computer vision*. Springer, 2020, pp. 206–222.

[81] P. Zhang, B. Zhang, D. Chen, L. Yuan, and F. Wen, “Cross-domain correspondence learning for exemplar-based image translation,” in *Conference on computer vision and pattern recognition*. IEEE, 2020, pp. 5143–5153.

[82] X. Zhou, B. Zhang, T. Zhang, P. Zhang, J. Bao, D. Chen, Z. Zhang, and F. Wen, “CoCosNet v2: Full-resolution correspondence learning for image translation,” in *Conference on computer vision and pattern recognition*. IEEE, 2021, pp. 11 465–11 475.

[83] A. Chen, R. Liu, L. Xie, Z. Chen, H. Su, and J. Yu, “Sofgan: A portrait image generator with dynamic styling,” *ACM Transactions on graphics*, vol. 41, no. 1, pp. 1–26, 2022.

[84] Y. Jing, Y. Yang, Z. Feng, J. Ye, Y. Yu, and M. Song, “Neural style transfer: A review,” *IEEE Transactions on visualization and computer graphics*, vol. 26, no. 11, pp. 3365–3385, 2019.

[85] Y. Chen, Y.-K. Lai, and Y.-J. Liu, “Cartoongan: Generative adversarial networks for photo cartoonization,” in *Conference on computer vision and pattern recognition*. IEEE, 2018, pp. 9465–9474.

[86] E. Richardson, Y. Alaluf, O. Patashnik, Y. Nitzan, Y. Azar, S. Shapiro, and D. Cohen-Or, “Encoding in style: a stylegan encoder for image-to-image translation,” in *Conference on computer vision and pattern recognition*. IEEE, 2021, pp. 2287–2296.

[87] L. A. Gatys, A. S. Ecker, and M. Bethge, “A neural algorithm of artistic style,” *arXiv preprint arXiv:1508.06576*, 2015.

[88] L. A. Gatys, A. S. Ecker, and M. Bethge, “Image style transfer using convolutional neural networks,” in *Conference on computer vision and pattern recognition*. IEEE, 2016, pp. 2414–2423.

[89] K. Simonyan and A. Zisserman, “Very deep convolutional networks for large-scale image recognition,” in *International Conference on Learning Representations*. OpenReview.net, 2015.

[90] T. Karras, S. Laine, and T. Aila, “A style-based generator architecture for generative adversarial networks,” in *Conference on computer vision and pattern recognition*. IEEE, 2019, pp. 4401–4410.

[91] R. Abdal, Y. Qin, and P. Wonka, “Image2styleGAN: How to embed images into the stylegan latent space?” in *International conference on computer vision*. IEEE, 2019, pp. 4432–4441.

[92] D. Kotovenko, M. Wright, A. Heimbrecht, and B. Ommer, “Rethinking style transfer: From pixels to parameterized brushstrokes,” in *Conference on computer vision and pattern recognition*. IEEE, 2021, pp. 12 196–12 205.

[93] J. Johnson, A. Alahi, and L. Fei-Fei, “Perceptual losses for real-time style transfer and super-resolution,” in *European conference on computer vision*. Springer, 2016, pp. 694–711.

[94] D. Ulyanov, V. Lebedev, A. Vedaldi, and V. S. Lempitsky, “Texture networks: Feed-forward synthesis of textures and stylized images,” in *International conference*

on machine learning. PMLR, 2016, p. 1349–1357.

[95] T. Q. Chen and M. Schmidt, “Fast patch-based style transfer of arbitrary style,” in *Advances in neural information processing systems workshops*. Curran Associates, Inc., 2016.

[96] M. Eitz, J. Hays, and M. Alexa, “How do humans sketch objects?” *ACM Transactions on graphics*, vol. 31, no. 4, pp. 1–10, 2012.

[97] T.-Y. Lin, M. Maire, S. Belongie, J. Hays, P. Perona, D. Ramanan, P. Dollár, and C. L. Zitnick, “Microsoft coco: Common objects in context,” in *European conference on computer vision*. Springer, 2014, pp. 740–755.

[98] O. Russakovsky, J. Deng, H. Su, J. Krause, S. Satheesh, S. Ma, Z. Huang, A. Karpathy, A. Khosla, M. Bernstein, A. C. Berg, and L. Fei-Fei, “ImageNet large scale visual recognition challenge,” *International journal of computer vision*, vol. 115, no. 3, pp. 211–252, 2015.

[99] M. Cimpoi, S. Maji, I. Kokkinos, S. Mohamed, and A. Vedaldi, “Describing textures in the wild,” in *Conference on computer vision and pattern recognition*. IEEE, 2014, pp. 3606–3613.

[100] S. Y. Duck, “Painter by numbers, [wikiart.org/](https://www.kaggle.com/c/painter-by-numbers),” <https://www.kaggle.com/c/painter-by-numbers>, 2016.

[101] M. Cordts, M. Omran, S. Ramos, T. Rehfeld, M. Enzweiler, R. Benenson, U. Franke, S. Roth, and B. Schiele, “The cityscapes dataset for semantic urban scene understanding,” in *Conference on computer vision and pattern recognition*. IEEE, 2016, pp. 3213–3223.

[102] R. Tyleček and R. Šára, “Spatial pattern templates for recognition of objects with regular structure,” in *German conference on pattern recognition*. Springer, 2013, pp. 364–374.

[103] J.-Y. Zhu, P. Krähenbühl, E. Shechtman, and A. A. Efros, “Generative visual manipulation on the natural image manifold,” in *European conference on computer vision*. Springer, 2016, pp. 597–613.

[104] A. Yu and K. Grauman, “Fine-grained visual comparisons with local learning,” in *Conference on computer vision and pattern recognition*. IEEE, 2014, pp. 192–199.

[105] P.-Y. Laffont, Z. Ren, X. Tao, C. Qian, and J. Hays, “Transient attributes for high-level understanding and editing of outdoor scenes,” *ACM Transactions on graphics*, vol. 33, no. 4, pp. 1–11, 2014.

[106] Y. LeCun, L. Bottou, Y. Bengio, and P. Haffner, “Gradient-based learning applied to document recognition,” *Proceedings of the IEEE*, vol. 86, no. 11, pp. 2278–2324, 1998.

[107] C. Wah, S. Branson, P. Welinder, P. Perona, and S. Belongie, “The caltech-ucsd birds-200-2011 dataset,” 2011.

[108] T. Karras, T. Aila, S. Laine, and J. Lehtinen, “Progressive growing of GANs for improved quality, stability, and variation,” in *International Conference on Learning Representations*. OpenReview.net, 2018.

[109] N. Silberman, D. Hoiem, P. Kohli, and R. Fergus, “Indoor segmentation and support inference from rgbd images,” in *European conference on computer vision*. Springer, 2012, pp. 746–760.

[110] B. Zhou, H. Zhao, X. Puig, S. Fidler, A. Barriuso, and A. Torralba, “Scene parsing through ade20k dataset,” in *Conference on computer vision and pattern recognition*. IEEE, 2017, pp. 633–641.

[111] Q. Yu, Y.-Z. Song, T. Xiang, and T. M. Hospedales, “Sketchx!-shoe/chair fine-grained SBIR dataset,” 2017.

- [112] D. Ha and D. Eck, “A neural representation of sketch drawings,” in *International Conference on Learning Representations*. OpenReview.net, 2018.
- [113] Y. Jin, J. Zhang, M. Li, Y. Tian, H. Zhu, and Z. Fang, “Towards the automatic anime characters creation with generative adversarial networks,” in *Advances in neural information processing systems workshops*. Curran Associates, Inc., 2017.
- [114] H. Xu, Y. Gao, F. Yu, and T. Darrell, “End-to-end learning of driving models from large-scale video datasets,” in *Conference on computer vision and pattern recognition*. IEEE, 2017, pp. 2174–2182.
- [115] G. Ros, L. Sellart, J. Materzynska, D. Vazquez, and A. M. Lopez, “The synthia dataset: A large collection of synthetic images for semantic segmentation of urban scenes,” in *Conference on computer vision and pattern recognition*. IEEE, 2016, pp. 3234–3243.
- [116] Z. Liu, P. Luo, S. Qiu, X. Wang, and X. Tang, “Deepfashion: Powering robust clothes recognition and retrieval with rich annotations,” in *Conference on computer vision and pattern recognition*. IEEE, 2016, pp. 1096–1104.
- [117] E. Agustsson and R. Timofte, “Ntire 2017 challenge on single image super-resolution: Dataset and study,” in *Conference on computer vision and pattern recognition workshops*. IEEE, 2017, pp. 126–135.
- [118] B. Yao, X. Yang, and S.-C. Zhu, “Introduction to a large-scale general purpose ground truth database: methodology, annotation tool and benchmarks,” in *CVPRW*. IEEE, 2007, pp. 169–183.
- [119] J. Krause, M. Stark, J. Deng, and L. Fei-Fei, “3d object representations for fine-grained categorization,” in *International conference on computer vision workshops*. IEEE, 2013, pp. 554–561.
- [120] F. Yu, A. Seff, Y. Zhang, S. Song, T. Funkhouser, and J. Xiao, “Lsun: Construction of a large-scale image dataset using deep learning with humans in the loop,” *arXiv preprint arXiv:1506.03365*, 2015.
- [121] V. Dumoulin, J. Shlens, and M. Kudlur, “A learned representation for artistic style,” in *International Conference on Learning Representations*. OpenReview.net, 2017.
- [122] D. Ulyanov, A. Vedaldi, and V. Lempitsky, “Improved texture networks: Maximizing quality and diversity in feed-forward stylization and texture synthesis,” in *Conference on computer vision and pattern recognition*. IEEE, 2017, pp. 6924–6932.
- [123] X. Huang and S. Belongie, “Arbitrary style transfer in real-time with adaptive instance normalization,” in *International conference on computer vision*. IEEE, 2017, pp. 1501–1510.
- [124] Y. Li, C. Fang, J. Yang, Z. Wang, X. Lu, and M.-H. Yang, “Universal style transfer via feature transforms,” in *Advances in neural information processing systems*. Curran Associates, Inc., 2017.
- [125] X. Huang, M.-Y. Liu, S. Belongie, and J. Kautz, “Multimodal unsupervised image-to-image translation,” in *European conference on computer vision*. Springer, 2018, pp. 172–189.
- [126] L. Zhang, L. Lin, X. Wu, S. Ding, and L. Zhang, “End-to-end photo-sketch generation via fully convolutional representation learning,” in *International Conference on Multimedia Retrieval*. ACM, 2015, pp. 627–634.
- [127] M. Zhu, N. Wang, X. Gao, and J. Li, “Deep graphical feature learning for face sketch synthesis,” in *International Joint Conference on Artificial Intelligence. IJCAI*, 2017, pp. 3574–3580.
- [128] P. Sangkloy, J. Lu, C. Fang, F. Yu, and J. Hays, “Scribbler: Controlling deep

image synthesis with sketch and color,” in *Conference on computer vision and pattern recognition*. IEEE, 2017, pp. 5400–5409.

[129] M. Zhang, N. Wang, Y. Li, R. Wang, and X. Gao, “Face sketch synthesis from coarse to fine,” in *AAAI Conference on Artificial Intelligence*. AAAI Press, 2018, pp. 7558–7565.

[130] W. Xian, P. Sangkloy, V. Agrawal, A. Raj, J. Lu, C. Fang, F. Yu, and J. Hays, “TextureGAN: Controlling deep image synthesis with texture patches,” in *Conference on computer vision and pattern recognition*. IEEE, 2018, pp. 8456–8465.

[131] J. Song, K. Pang, Y.-Z. Song, T. Xiang, and T. M. Hospedales, “Learning to sketch with shortcut cycle consistency,” in *Conference on computer vision and pattern recognition*. IEEE, 2018, pp. 801–810.

[132] Y. Lu, S. Wu, Y.-W. Tai, and C.-K. Tang, “Image generation from sketch constraint using contextual GAN,” in *European conference on computer vision*. Springer, 2018, pp. 205–220.

[133] S. Zhang, R. Ji, J. Hu, Y. Gao, and C.-W. Lin, “Robust face sketch synthesis via generative adversarial fusion of priors and parametric sigmoid,” in *International Joint Conference on Artificial Intelligence*. IJCAI, 2018, pp. 1163–1169.

[134] M. Zhang, N. Wang, X. Gao, and Y. Li, “Markov random neural fields for face sketch synthesis,” in *International Joint Conference on Artificial Intelligence*. IJCAI, 2018, pp. 1142–1148.

[135] L. Wang, V. Sindagi, and V. Patel, “High-quality facial photo-sketch synthesis using multi-adversarial networks,” in *International conference on automatic face & gesture recognition*. IEEE, 2018, pp. 83–90.

[136] M. Zhang, R. Wang, X. Gao, J. Li, and D. Tao, “Dual-transfer face sketch-photo synthesis,” *IEEE Transactions on image processing*, vol. 28, no. 2, pp. 642–657, 2018.

[137] H. Kazemi, M. Iranmanesh, A. Dabouei, S. Soleymani, and N. M. Nasrabadi, “Facial attributes guided deep sketch-to-photo synthesis,” in *Winter Applications of Computer Vision Workshops*. IEEE, 2018, pp. 1–8.

[138] H. Kazemi, F. Taherkhani, and N. M. Nasrabadi, “Unsupervised facial geometry learning for sketch to photo synthesis,” in *International Conference of the Biometrics Special Interest Group*. IEEE, 2018, pp. 1–5.

[139] S. You, N. You, and M. Pan, “Pi-rec: Progressive image reconstruction network with edge and color domain,” *arXiv preprint arXiv:1903.10146*, 2019.

[140] M. Zhang, N. Wang, Y. Li, and X. Gao, “Deep latent low-rank representation for face sketch synthesis,” *IEEE Transactions on Neural Networks and Learning Systems*, vol. 30, no. 10, pp. 3109–3123, 2019.

[141] M. Zhu, J. Li, N. Wang, and X. Gao, “A deep collaborative framework for face photo-sketch synthesis,” *IEEE Transactions on Neural Networks and Learning Systems*, vol. 30, no. 10, pp. 3096–3108, 2019.

[142] M. Zhang, Y. Li, N. Wang, Y. Chi, and X. Gao, “Cascaded face sketch synthesis under various illuminations,” *IEEE Transactions on image processing*, vol. 29, pp. 1507–1521, 2019.

[143] M. Zhu, N. Wang, X. Gao, J. Li, and Z. Li, “Face photo-sketch synthesis via knowledge transfer,” in *International Joint Conference on Artificial Intelligence*. IJCAI, 2019, pp. 1048–1054.

[144] Y. Li, C. Fang, A. Hertzmann, E. Shechtman, and M.-H. Yang, “Im2pencil: Controllable pencil illustration from photographs,” in *Conference on computer vision and pattern recognition*. IEEE, 2019, pp. 1525–1534.

[145] A. Ghosh, R. Zhang, P. K. Dokania, O. Wang, A. A. Efros, P. H. Torr, and E. Shechtman, “Interactive sketch & fill: Multiclass sketch-to-image translation,” in *International conference on computer vision*. IEEE, 2019, pp. 1171–1180.

[146] X. Wang and J. Yu, “Learning to cartoonize using white-box cartoon representations,” in *Conference on computer vision and pattern recognition*. IEEE, 2020, pp. 8090–8099.

[147] C. Gao, Q. Liu, Q. Xu, L. Wang, J. Liu, and C. Zou, “Sketchycoco: image generation from freehand scene sketches,” in *Conference on computer vision and pattern recognition*. IEEE, 2020, pp. 5174–5183.

[148] S. Yang, Z. Wang, J. Liu, and Z. Guo, “Deep plastic surgery: Robust and controllable image editing with human-drawn sketches,” in *European conference on computer vision*. Springer, 2020, pp. 601–617.

[149] S.-Y. Chen, W. Su, L. Gao, S. Xia, and H. Fu, “DeepFaceDrawing: Deep generation of face images from sketches,” *ACM Transactions on graphics*, vol. 39, no. 4, pp. 72–1, 2020.

[150] J. Yu, X. Xu, F. Gao, S. Shi, M. Wang, D. Tao, and Q. Huang, “Toward realistic face photo-sketch synthesis via composition-aided gans,” *IEEE Transactions on cybernetics*, vol. 51, no. 9, pp. 4350–4362, 2020.

[151] Y. Fang, W. Deng, J. Du, and J. Hu, “Identity-aware CycleGAN for face photo-sketch synthesis and recognition,” *Pattern Recognition*, vol. 102, p. 107249, 2020.

[152] Y. Lin, S. Ling, K. Fu, and P. Cheng, “An identity-preserved model for face sketch-photo synthesis,” *IEEE Signal Processing Letters*, vol. 27, pp. 1095–1099, 2020.

[153] C. Peng, N. Wang, J. Li, and X. Gao, “Universal face photo-sketch style transfer via multiview domain translation,” *IEEE Transactions on image processing*, vol. 29, pp. 8519–8534, 2020.

[154] S. Duan, Z. Chen, Q. J. Wu, L. Cai, and D. Lu, “Multi-scale gradients self-attention residual learning for face photo-sketch transformation,” *IEEE Transactions on Information Forensics and Security*, vol. 16, pp. 1218–1230, 2020.

[155] S.-Y. Wang, D. Bau, and J.-Y. Zhu, “Sketch your own GAN,” in *International conference on computer vision*. IEEE, 2021, pp. 14 050–14 060.

[156] A. K. Bhunia, S. Khan, H. Cholakkal, R. M. Anwer, F. S. Khan, J. Laaksonen, and M. Felsberg, “Doodleformer: Creative sketch drawing with transformers,” *arXiv preprint arXiv:2112.03258*, 2021.

[157] Y. Song, C. Yang, Y. Shen, P. Wang, Q. Huang, and C.-C. J. Kuo, “Spg-net: Segmentation prediction and guidance network for image inpainting,” in *British Machine Vision Conference*. BMVA Press, 2018, p. 97.

[158] D. Yi, Z. Lei, S. Liao, and S. Z. Li, “Learning face representation from scratch,” *arXiv preprint arXiv:1411.7923*, 2014.

[159] L. Wang, R.-F. Li, K. Wang, and J. Chen, “Feature representation for facial expression recognition based on facs and lbp,” *International Journal of Automation and Computing*, vol. 11, no. 5, pp. 459–468, 2014.

[160] X. Zheng, Y. Guo, H. Huang, Y. Li, and R. He, “A survey of deep facial attribute analysis,” *International journal of computer vision*, vol. 128, no. 8, pp. 2002–2034, 2020.

[161] G. B. Huang, M. Mattar, T. Berg, and E. Learned-Miller, “Labeled faces in the wild: A database for studying face recognition in unconstrained environments,” in *Workshop on faces in 'Real-Life' Images: detection, alignment, and recognition*, 2008.

[162] R. Ranjan, V. M. Patel, and R. Chellappa, “Hyperface: A deep multi-task learning framework for face detection, landmark localization, pose estimation, and gender recognition,” *IEEE Transactions on pattern analysis and machine intelligence*, vol. 41, no. 1, pp. 121–135, 2017.

[163] E. M. Hand and R. Chellappa, “Attributes for improved attributes: A multi-task network utilizing implicit and explicit relationships for facial attribute classification,” in *AAAI Conference on Artificial Intelligence*. AAAI Press, 2017, pp. 4068–4074.

[164] H. Han, A. K. Jain, F. Wang, S. Shan, and X. Chen, “Heterogeneous face attribute estimation: A deep multi-task learning approach,” *IEEE Transactions on pattern analysis and machine intelligence*, vol. 40, no. 11, pp. 2597–2609, 2017.

[165] Y. Jang, H. Gunes, and I. Patras, “Smilenet: registration-free smiling face detection in the wild,” in *International conference on computer vision workshops*. IEEE, 2017, pp. 1581–1589.

[166] R. Ranjan, S. Sankaranarayanan, C. D. Castillo, and R. Chellappa, “An all-in-one convolutional neural network for face analysis,” in *International conference on automatic face & gesture recognition*. IEEE, 2017, pp. 17–24.

[167] S. Li and W. Deng, “Deep facial expression recognition: A survey,” *Transactions on affective computing*, 2020.

[168] N. Zhang, M. Paluri, M. Ranzato, T. Darrell, and L. Bourdev, “Panda: Pose aligned networks for deep attribute modeling,” in *Conference on computer vision and pattern recognition*. IEEE, 2014, pp. 1637–1644.

[169] M. Kan, S. Shan, H. Chang, and X. Chen, “Stacked progressive auto-encoders (spae) for face recognition across poses,” in *Conference on computer vision and pattern recognition*. IEEE, 2014, pp. 1883–1890.

[170] Y. Wu, Z. Wang, and Q. Ji, “Facial feature tracking under varying facial expressions and face poses based on restricted boltzmann machines,” in *Conference on computer vision and pattern recognition*. IEEE, 2013, pp. 3452–3459.

[171] L. Tran, X. Yin, and X. Liu, “Disentangled representation learning GAN for pose-invariant face recognition,” in *Conference on computer vision and pattern recognition*. IEEE, 2017, pp. 1415–1424.

[172] U. Toseeb, D. R. Keeble, and E. J. Bryant, “The significance of hair for face recognition,” *PLoS one*, vol. 7, no. 3, p. e34144, 2012.

[173] S. J. Bartel, K. Toews, L. Gronhovd, and S. L. Prime, “Do i know you? altering hairstyle affects facial recognition,” *Visual Cognition*, vol. 26, no. 3, pp. 149–155, 2018.

[174] N. Kumar, P. Belhumeur, and S. Nayar, “Facetracer: A search engine for large collections of images with faces,” in *European conference on computer vision*. Springer, 2008, pp. 340–353.

[175] L. Huai-Yu, D. Wei-Ming, and B.-G. Hu, “Facial image attributes transformation via conditional recycle generative adversarial networks,” *Journal of Computer Science and Technology*, vol. 33, no. 3, pp. 511–521, 2018.

[176] J.-S. Pierrard and T. Vetter, “Skin detail analysis for face recognition,” in *Conference on computer vision and pattern recognition*. IEEE, 2007, pp. 1–8.

[177] S. Z. Li, *Encyclopedia of Biometrics: I-Z*. Springer Science & Business Media, 2009, vol. 2.

[178] K. Zhang, Z. Zhang, Z. Li, and Y. Qiao, “Joint face detection and alignment using multitask cascaded convolutional networks,” *IEEE Signal Processing Letters*, vol. 23, no. 10, pp. 1499–1503, 2016.

- [179] K. He, X. Zhang, S. Ren, and J. Sun, “Deep residual learning for image recognition,” in *Conference on computer vision and pattern recognition*. IEEE, 2016, pp. 770–778.
- [180] Y. Choi, M. Choi, M. Kim, J.-W. Ha, S. Kim, and J. Choo, “StarGAN: Unified generative adversarial networks for multi-domain image-to-image translation,” in *Conference on computer vision and pattern recognition*. IEEE, 2018, pp. 8789–8797.
- [181] B. Zhao, B. Chang, Z. Jie, and L. Sigal, “Modular generative adversarial networks,” in *European conference on computer vision*. Springer, 2018, pp. 150–165.
- [182] A. Paszke, S. Gross, S. Chintala, G. Chanan, E. Yang, Z. DeVito, Z. Lin, A. Desmaison, L. Antiga, and A. Lerer, “Automatic differentiation in pytorch,” in *Advances in neural information processing systems workshops*. Curran Associates, Inc., 2017.
- [183] D. P. Kingma and J. Ba, “Adam: A method for stochastic optimization,” in *International Conference on Learning Representations*. OpenReview.net, 2014.
- [184] Q. Yu, F. Liu, Y.-Z. Song, T. Xiang, T. M. Hospedales, and C.-C. Loy, “Sketch me that shoe,” in *Conference on computer vision and pattern recognition*. IEEE, 2016, pp. 799–807.
- [185] C. Shorten and T. M. Khoshgoftaar, “A survey on image data augmentation for deep learning,” *Journal of big data*, vol. 6, no. 1, pp. 1–48, 2019.
- [186] Y. Wang, C. Wu, L. Herranz, J. van de Weijer, A. Gonzalez-Garcia, and B. Raducanu, “Transferring gans: generating images from limited data,” in *ECCV*. Springer, 2018, pp. 218–234.
- [187] L. Yu, J. van de Weijer *et al.*, “Deepi2i: Enabling deep hierarchical image-to-image translation by transferring from gans,” in *Advances in neural information processing systems*. Curran Associates, Inc., 2020.
- [188] A. Shocher, Y. Gandelsman, I. Mosseri, M. Yarom, M. Irani, W. T. Freeman, and T. Dekel, “Semantic pyramid for image generation,” in *International conference on computer vision*. IEEE, 2020, pp. 7457–7466.
- [189] S. Ravi and H. Larochelle, “Optimization as a model for few-shot learning,” in *International Conference on Learning Representations*. OpenReview.net, 2017.
- [190] O. Chapelle, B. Scholkopf, and A. Zien, “Semi-supervised learning (chapelle, o. et al., eds.; 2006)[book reviews],” *IEEE Transactions on Neural Networks*, vol. 20, no. 3, pp. 542–542, 2009.
- [191] M. Oquab, L. Bottou, I. Laptev, and J. Sivic, “Is object localization for free? - weakly-supervised learning with convolutional neural networks,” in *Conference on computer vision and pattern recognition*. IEEE, 2015, pp. 685–694.
- [192] X. Wang, K. He, and A. Gupta, “Transitive invariance for self-supervised visual representation learning,” in *International conference on computer vision*. IEEE, 2017, pp. 1329–1338.
- [193] R. Pinto, T. Mettler, and M. Taisch, “Managing supplier delivery reliability risk under limited information: Foundations for a human-in-the-loop DSS,” *Decision support systems*, vol. 54, no. 2, pp. 1076–1084, 2013.
- [194] Y. LeCun *et al.*, “Generalization and network design strategies,” *Connectionism in perspective*, vol. 19, no. 143–155, p. 18, 1989.
- [195] I. O. Tolstikhin, N. Houlsby, A. Kolesnikov, L. Beyer, X. Zhai, T. Unterthiner, J. Yung, A. Steiner, D. Keysers, J. Uszkoreit *et al.*, “Mlp-mixer: An all-mlp architecture for vision,” in *Advances in neural information processing systems*. Curran Associates, Inc., 2021.
- [196] A. Vaswani, N. Shazeer, N. Parmar, J. Uszkoreit, L. Jones, A. N. Gomez,

L. Kaiser, and I. Polosukhin, “Attention is all you need,” in *Advances in neural information processing systems*. Curran Associates, Inc., 2017.

- [197] K. Lee, H. Chang, L. Jiang, H. Zhang, Z. Tu, and C. Liu, “ViTGAN: Training GANs with vision transformers,” in *International Conference on Learning Representations*. OpenReview.net, 2022.
- [198] L. Zhang, L. Zhang, X. Mou, and D. Zhang, “Fsim: A feature similarity index for image quality assessment,” *IEEE Transactions on image processing*, vol. 20, no. 8, pp. 2378–2386, 2011.
- [199] S. Avidan and A. Shamir, “Seam carving for content-aware image resizing,” *ACM Transactions on graphics*, vol. 26, no. 3, p. 10–es, 2007.
- [200] C. Dong, C. C. Loy, K. He, and X. Tang, “Image super-resolution using deep convolutional networks,” *IEEE Transactions on pattern analysis and machine intelligence*, vol. 38, no. 2, pp. 295–307, 2015.
- [201] Y. Hu, S. Yang, W. Yang, L.-Y. Duan, and J. Liu, “Towards coding for human and machine vision: A scalable image coding approach,” in *IEEE International Conference on Multimedia and Expo*. IEEE, 2020, pp. 1–6.
- [202] E. Wood, T. Baltrušaitis, C. Hewitt, S. Dziadzio, T. J. Cashman, and J. Shotton, “Fake it till you make it: Face analysis in the wild using synthetic data alone,” in *International conference on computer vision*. IEEE, 2021, pp. 3681–3691.